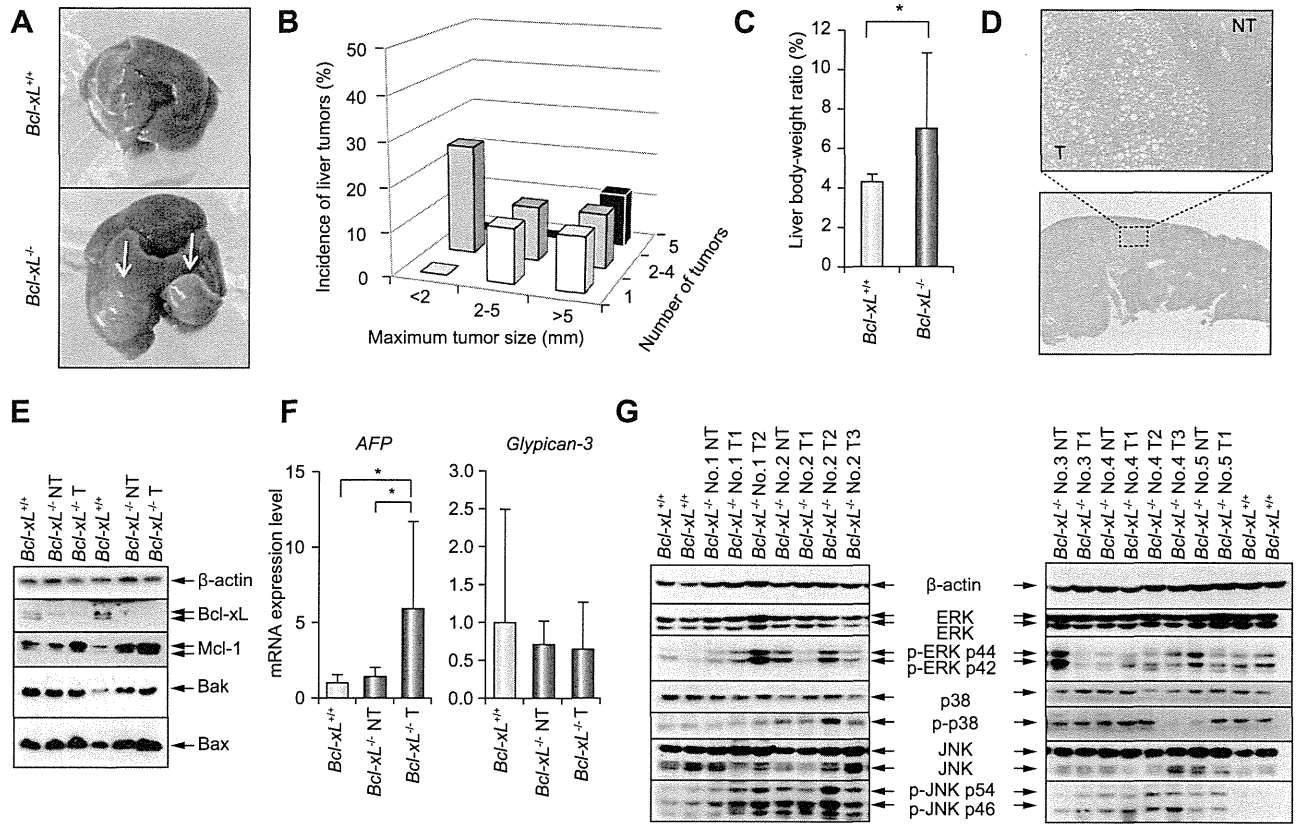

Fig. 1. Liver tumors in *Bcl-xL* KO mice. (A–E) Hepatocyte-specific *Bcl-xL*-deficient mice (*Bcl-xL*$^{-/-}$) (N = 8) and their control littermates (*Bcl-xL*$^{+/+}$) (N = 10) were sacrificed at 1.5 years of age. (A) Representative macroscopic view of the livers with arrows indicating tumors. (B) Incidence of liver tumors separated by maximum tumor size and number of tumors. (C) Liver body-weight ratio. (D) Representative histology of liver tumors in *Bcl-xL* KO mice. (E) Western blot of the Bcl-2 family proteins in tumors (T) and surrounding non-cancerous livers (NT) of *Bcl-xL* KO mice and livers of control mice. (F and G) Characteristics of liver tumors in *Bcl-xL* KO mice. (F) Real-time RT-PCR analysis of the expression levels of α-fetoprotein (*AFP*) and *glypican-3* mRNA (N = 9 or 10 per group). (G) Expression and activation of mitogen-activated protein kinases. *p <0.05.

and Table 1). As in the case of tumors of *Bcl-xL* KO mice, liver tumors that developed in *Mcl-1* KO mice were deficient for Mcl-1 expression and, in most cases, reciprocally overexpressed Bcl-xL (Fig. 2E and Supplementary Fig. 2B). These tumors expressed higher levels of α-fetoprotein and glypican-3 (Fig. 2F) and frequently showed activation of ERK and JNK (Fig. 2G).

Inflammatory response and oxidative stress occur in Bcl-xL- or Mcl-1-KO livers

To examine the molecular mechanism of tumor development, we examined gene expression in the livers of 6-week-old *Bcl-xL* or *Mcl-1* KO mice. Real-time RT-PCR analysis revealed increases of inflammatory cytokine TNF-α, but not IL-6, and chemokine MCP-1 in *Bcl-xL* and *Mcl-1* KO livers (Fig. 3A and B), despite overt histological inflammation (data not shown). Together with an increase of MCP-1, CD68 expression was significantly higher in KO livers than in control livers (Fig. 3C and D). In contrast, there was no difference in the expression of CD4 and CD8 between the groups. These findings suggest that activation or infiltration of myeloid-derived cells and production of TNF-α are characteristic of the *Bcl-xL* or *Mcl-1* KO liver. Together with the previous study reporting that TNF-α promotes cellular transformation [20], these results suggest that the increase in TNF-α may be one of the mechanisms of tumor development.

Since oxidative stress is also reported to cause carcinogenesis [21], we examined the expression of HO-1 and NQO1, inducible anti-oxidant enzymes, and 8-OHdG in the liver tissues. Real-time RT-PCR analysis revealed that HO-1 and NQO-1 expressions were significantly increased in *Mcl-1* KO livers at 6 weeks (Fig. 3E). 8-OHdG staining revealed that there were few 8-OHdG positive nuclei in both *Mcl-1* KO and the control liver at 6 weeks of age. However, scattered positive nuclei were observed in KO livers at 1.5 years of age, but not in the tumors, and the number of positive nuclei was significantly higher in KO livers than in control livers (Fig. 3F and Supplementary Fig. 3). Similarly, the number of 8-OHdG positive nuclei was significantly higher in *Bcl-xL* KO livers at 1.5 years of age than in control livers (Fig. 3G). These results suggest that oxidative stress may occur at as early as 6 weeks of age in KO livers and that oxidative injury arises at a later time point.

Bak deficiency significantly ameliorates hepatocyte apoptosis and reduces tumor development in Mcl-1 KO mice

Bak is a proapoptotic Bcl-2 family protein, which is able to oligmerize to form pores at the outer membrane of mitochondria. To understand whether inhibition of apoptosis could reduce the carcinogenic potential, we crossed *Mcl-1* KO mice and *Bak* KO mice and generated *Bak Mcl-1* double KO mice. As expected, *Bak* KO significantly suppressed hepatocyte apoptosis in *Mcl-1*

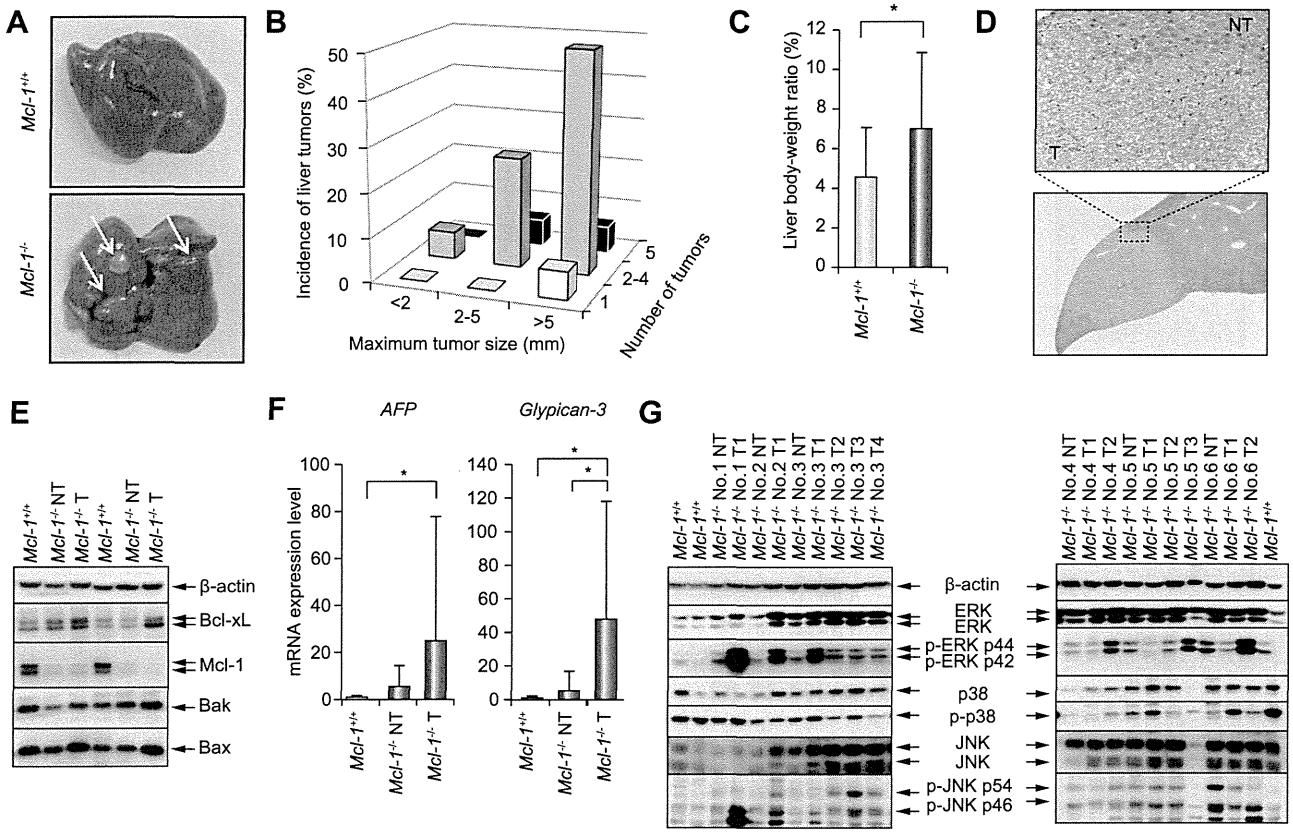

Fig. 2. Liver tumors in *Mcl-1* KO mice. (A–E) Hepatocyte-specific *Mcl-1*-deficient mice (*Mcl-1*$^{-/-}$) (N = 16) and their control littermates (*Mcl-1*$^{+/+}$) (N = 22) were sacrificed at 1.5 years of age. (A) Representative macroscopic view of the livers with arrows indicating tumors. (B) Incidence of liver tumors separated by maximum tumor size and number of tumors. (C) Liver body-weight ratio. (D) Representative histology of liver tumors in *Mcl-1* KO mice. (E) Western blot of the Bcl-2 family proteins in tumors (T) and surrounding non-cancerous livers (NT) of *Mcl-1* KO mice and livers of control mice. (F and G) Characteristics of liver tumors in *Mcl-1* KO mice. (F) Real-time RT-PCR analysis of the expression levels of α-fetoprotein (*AFP*) and *glypican-3* mRNA (N = 16 per group). (G) Expression and activation of mitogen-activated protein kinases. *p <0.05.

KO mice as evidenced by TUNEL staining of liver sections, serum ALT levels and caspase-3/7 activity at 6 weeks of age (Fig. 4A–C). Weber *et al.* [12] previously described hepatocyte regeneration in the *Mcl-1* KO liver. In agreement with this, *Mcl-1* KO livers showed higher expression of cell cycle markers PCNA and ki-67, than those from control littermates (Fig. 4A, B, and D and Supplementary Fig. 4). Importantly, the levels of PCNA and ki-67 expression decreased with a *Bak* KO background in *Mcl-1* KO mice. While *Mcl-1* KO livers show a mild fibrotic change [11], the levels of col1a1 expression at 6 weeks of age and Sirius red staining at 1 year of age decreased with a *Bak* KO background in *Mcl-1* KO livers (Fig. 4E and Supplementary Fig. 5). Bak deficiency also reduced expression levels of TNF-α, MCP-1, and CD68 at 6 weeks of age (Fig. 4F). Next, we examined the impact of apoptosis inhibition by Bak deficiency on oxidative stress markers, which were increased in *Mcl-1* KO livers. Real-time RT-PCR revealed that Bak deficiency reduced the levels of HO-1 and NQO1 expression at 6 weeks of age (Fig. 4G). Consistent with these observations, *Bak* KO significantly lowered the number of 8-OHdG-positive nuclei in *Mcl-1* KO livers at 1 year of age (Fig. 4H). These results suggested that inhibition of hepatocyte apoptosis reduced oxidative stress in the liver. Finally, to examine the impact of apoptosis inhibition on liver tumor development, we compared the carcinogenetic rates in *Mcl-1* KO mice with or without *Bak* KO background at 1 year of age and found that *Bak* KO significantly suppressed liver tumor development (Fig. 5A and B and Table 1).

Discussion

Mcl-1 was first identified as a gene induced during myeloid cell differentiation. Compared with other anti-apoptotic members such as Bcl-2, Bcl-xL, Bcl-w, and Bfl-1, Mcl-1 possesses a unique N-terminus containing two PEST domains, which are found in proteins displaying rapid turnover, and its expression is tightly regulated by growth factors and a variety of other stimuli. Mice systemically deficient for Bcl-xL suffered embryonic death due to massive apoptosis in hematopoietic organs and developing neurons [22]. On the other hand, systemic *Mcl-1* KO resulted in peri-implantation lethality, but *Mcl-1* KO embryos showed no alterations in the extent of apoptosis [23], suggesting that Mcl-1 may play a role early in development that is distinct from its anti-apoptotic functions. Indeed, *in vitro* studies have shown that Mcl-1 interacts with PCNA and Cdk1 in the nucleus and inhibits proliferation [13,14]. Recently, the early responding gene *IEX-1*

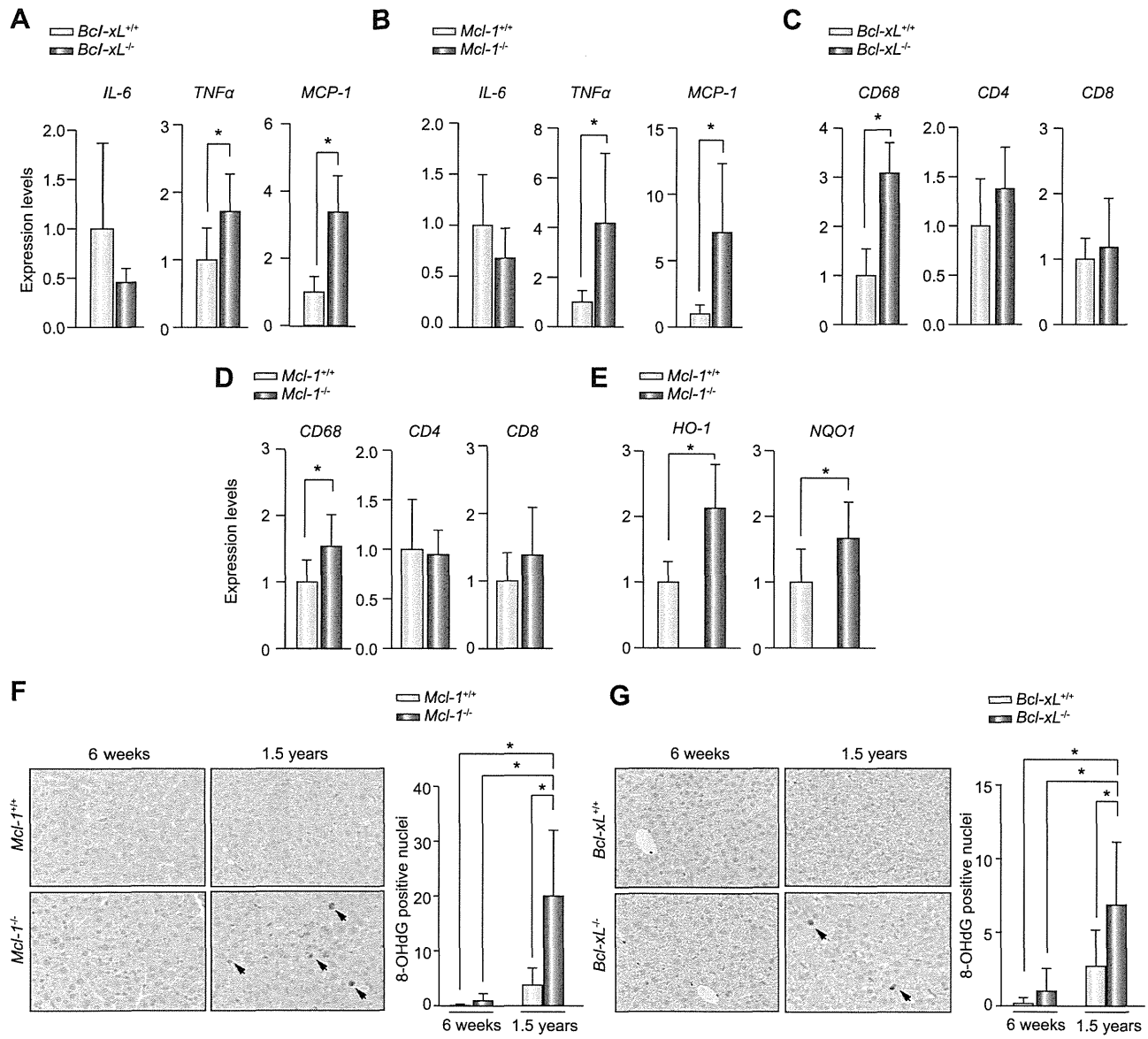

Fig. 3. Inflammatory response and oxidative stress in *Bcl-xL* or *Mcl-1* KO liver. (A–D) Inflammatory responses in KO livers. (A and C) Hepatocyte-specific *Bcl-xL* KO mice (*Bcl-xL*$^{-/-}$) and their control littermates (*Bcl-xL*$^{+/+}$) (N = 6 per group) as well as (B and D) hepatocyte-specific *Mcl-1* KO (*Mcl-1*$^{-/-}$) mice and their control littermates (*Mcl-1*$^{+/+}$) (N = 9 per group) were sacrificed at 6 weeks of age. Expression levels of (A and B) inflammatory molecules and (C and D) cell surface markers of immune cells were analyzed by real-time RT-PCR. (E–G) Oxidative injury in KO livers. (E) Real-time RT-PCR analysis of the expression levels of *HO-1* and *NQO1* of *Mcl-1* KO and control livers at 6 weeks of age (N = 9 per group). (F) Liver sections of *Mcl-1* KO or (G) *Bcl-xL* KO and the control liver at the indicated ages stained with anti-8-OHdG and statistics of the number of positive nuclei (N = 6 and more per group) (G). *p <0.05.

was found to be induced upon DNA damage and to be bound to and to transport Mcl-1 from the cytosol to the nucleus [15]. Mcl-1 was also reported to be induced upon DNA damage and to regulate the DNA damage response through activation of Chk1 [16]. These findings suggest that Mcl-1 possesses additional functions in cell cycle progression and the DNA damage response pathway. This raised concern as to whether the hepatocarcinogenesis observed in *Mcl-1* KO mice was actually related to increased apoptosis in the liver.

In the present study, we demonstrated that hepatocyte-specific destruction of Bcl-xL led to the development of liver cancer similarly to that in hepatocyte-specific *Mcl-1* KO mice. Although we could not completely exclude the possibility that Bcl-xL may have additional effects other than apoptosis, this finding clearly shows that hepatocarcinogenesis observed in the apoptosis-prone liver is not a specific finding of loss of Mcl-1 but is also observed with the knockout of other genes that are critically involved in hepatocyte integrity. Tumors observed in these murine livers frequently showed activation of ERK and JNK, similar to the activation observed in human HCC [18,19]. While 64% of *Mcl-1* KO mice (14/22) developed liver tumors within 1 year, only 27% of *Bcl-xL* KO mice (3/11) did so within 1 year (Table 1). These finding indicate that the incidence rate of carcinogenesis in *Bcl-xL* KO mice is lower than that of *Mcl-1* KO mice. This may be

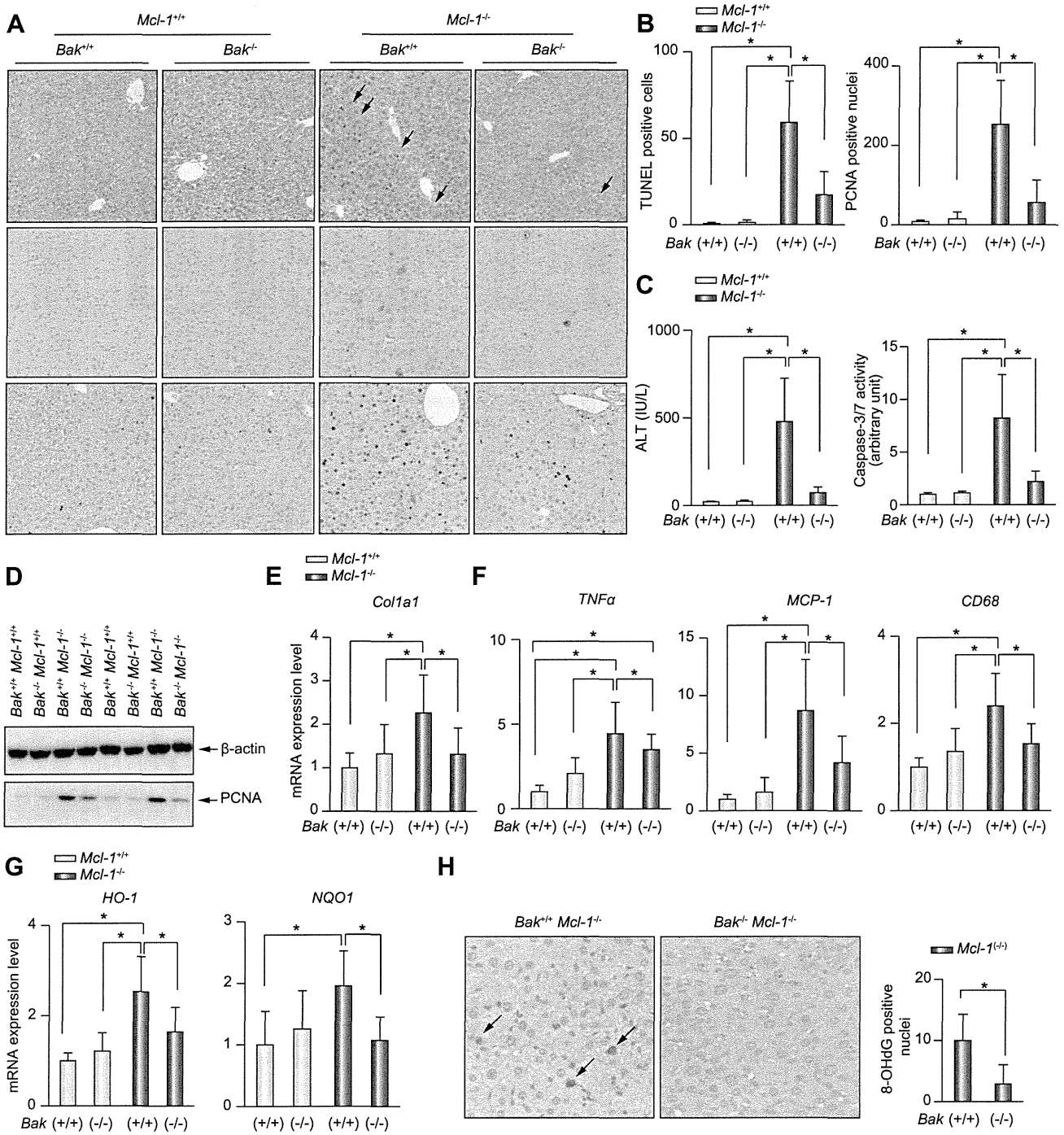

Fig. 4. Impact of Bak deficiency in *Mcl-1* KO mice. (A–G) *Bak*-deficient hepatocyte-specific *Mcl-1* KO mice ($Bak^{-/-}$ $Mcl\text{-}1^{-/-}$) were sacrificed at 6 weeks of age. (A) Representative pictures of hematoxylin–eosin with arrows indicating typical apoptotic cells (upper), TUNEL (middle) and PCNA staining (lower) and (B) statistics of TUNEL and PCNA staining of liver sections (N = 6 or 8 per group). (C) Serum levels of ALT and caspase-3/7 activity (N = 12 per group). (D) Western blot for PCNA expression. Real-time RT-PCR analysis for expression levels of (E) *Col1a1*, (F) *TNF-α*, *MCP-1*, *CD68*, (G) *HO-1* and *NQO1* in the livers at 6 weeks of age (N = 12 per group). (H) Liver sections of the *Bak*-deficient *Mcl-1* KO and control *Mcl-1* KO liver at 1 year of age stained with anti-8-OHdG. Representative images of liver sections stained with anti-8-OHdG (left) and statistics of the number of positive nuclei (N = 9 or 7 per group) (right). *$p < 0.05$.

explained by the difference in levels of hepatocyte apoptosis and serum ALT, which are higher in *Mcl-1* KO mice than in *Bcl-xL* KO mice of the same age [10,11].

Mcl-1 executes its anti-apoptotic function by either directly or indirectly inhibiting the pro-apoptotic functions of Bak and/or Bax [24]. In the present study, we have shown that deletion of the *bak*

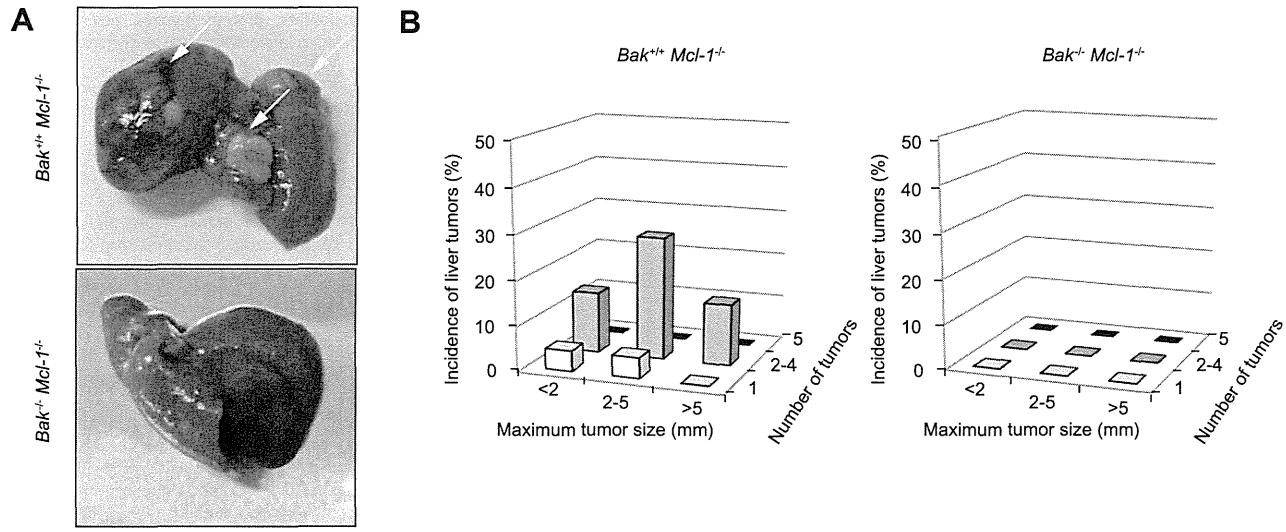

Fig. 5. Liver of aged *Bak/Mcl-1* double KO mice. (A and B) *Bak*-deficient *Mcl-1* KO mice ($Bak^{-/-}$ $Mcl\text{-}1^{-/-}$) (N = 7) and control *Mcl-1* KO mice ($Bak^{+/+}$ $Mcl\text{-}1^{-/-}$) (N = 22) were sacrificed at 1 year of age. (A) Representative macroscopic view of the livers with arrows indicating tumors. (B) Incidence of liver tumors separated by maximum tumor size and number of tumors.

gene resulted in a clear reduction in hepatocyte apoptosis in *Mcl-1* KO mice. Of importance is the finding that *bak* deletion leads to reduction of the liver regenerative response in *Mcl-1* KO mice. Bak is exclusively localized at the mitochondria in hepatocytes [25] and, upon exposure to apoptotic stimuli, undergoes oligomerization to form pores in the outer membrane of mitochondria, releasing cytochrome c, which in turn activates caspases. Since Bak is not involved in the activity of Mcl-1 in the nucleus, our present finding suggests that the regeneration observed in the *Mcl-1* KO liver is not due to loss of the Mcl-1 anti-proliferative effect but mainly to the compensatory regeneration of increased apoptosis. Most importantly, *bak* deletion clearly leads to reduced liver tumor incidence. This finding strongly suggests that the hepatocarcinogenesis observed in *Mcl-1* KO mice can be mostly ascribed to increased apoptosis in hepatocytes.

What does make hepatocytes undergo malignant transformation in the liver with increasing apoptosis? Regeneration is a physiological process in the liver like that in bone marrow or the intestine and compensatory liver regeneration itself is probably not sufficient to induce liver cancer [26]. The present study raised the possibility that TNF-α and oxidative stress are candidate factors responsible for the malignant transformation in the apoptosis-prone liver. TNF-α is reported to be a potent endogenous mutagen that promotes cellular transformation [20], and oxidative stress is reported to cause DNA damage leading to carcinogenesis [21]. Our results revealed that both TNF-α and oxidative stress were significantly increased in KO livers, and importantly, that inhibition of apoptosis by deletion of the *bak* gene reduced the levels of TNF-α and oxidative stress with a decrease in the tumorigenic rate. Some studies have shown that TNF-α induces oxidative stress in hepatocytes [27,28], while oxidative stress promotes production of inflammatory cytokines [29–31]. Taken together, oxidative stress and inflammatory cytokines may positively affect each other to turn healthy hepatocytes into malignant transformed hepatocytes in the liver of KO mice. Further studies are needed to examine the role of oxidative stress and inflammatory cytokines in apoptosis-induced hepatocarcinogenesis.

Apoptosis resistance has been established as a hallmark of cancer [32]. Indeed, accumulating evidence indicates that human HCC frequently overexpresses a variety of molecules which confer apoptosis resistance, such as anti-apoptotic Bcl-2 family proteins, Bcl-xL [33] and Mcl-1 [34,35]. Their overexpression was found to be associated with malignant phenotypes of tumors and poor prognosis of patients [36]. In the present study, tumors that developed in *Bcl-xL* or *Mcl-1* KO mice lacked expression of the respective proteins but reciprocally overexpressed Mcl-1 or Bcl-xL at high rates. We recently reported that conditional expression of Bcl-xL in tumor cells was translated into higher tumor growth in xenograft models [37], indicating that overexpression of anti-apoptotic Bcl-2 family proteins is important for tumor progression. Lack of Bcl-xL or Mcl-1 in hepatocytes generates persistent hepatocyte apoptosis leading to liver tumor development. On the other hand, reciprocal overexpression of Mcl-1 or Bcl-xL in the tumor of *Bcl-xL* or *Mcl-1* KO mice might be required for tumor progression.

Increasing evidence indicates that the serum level of ALT, a marker of hepatocyte apoptosis, is a risk factor for HCC in viral hepatitis [38] and non-alcoholic steatohepatitis [39]. A population-based study also revealed that elevated ALT levels raise the risk of liver cancer [40]. The present study provides evidence that spontaneous apoptosis in hepatocytes leads to liver cancer development and also offers genetic evidence that inhibition of apoptosis can help prevent liver cancer. Administration of caspase inhibitor was previously reported to lower serum ALT levels in patients with chronic hepatitis C [41]. It may be interesting and important, from a clinical point of view, to further determine whether pharmacological inhibition of apoptosis can be useful in preventing liver cancer development in *Bcl-xL* or *Mcl-1* KO mice.

Financial support

This work was partly supported by a Grant-in-Aid for Scientific Research from the Ministry of Education, Culture, Sports, Science, and Technology, Japan (to T. Tak.) and a Grant-in-Aid for Research

on Hepatitis from the Ministry of Health, Labour, and Welfare of Japan.

Conflict of interest

The authors who have taken part in this study declared that they do not have anything to disclose regarding funding or conflict of interest with respect to this manuscript.

Acknowledgements

We sincerely thank Dr. You-Wen He (Department of Immunology, Duke University Medical Center, Durham, NC) for providing the *mcl-1* floxed mice and Dr. Lothar Hennighausen (Laboratory of Genetics and Physiology, National Institute of Diabetes and Digestive and Kidney Diseases, National Institute of Health, Bethesda, MD) for providing the *Bcl-x* floxed mice.
This work was partly supported by a Grant-in-Aid for Scientific Research from the Ministry of Education, Culture, Sports, Science, and Technology, Japan (to T. Tak.) and Grant-in-Aid for Research on Hepatitis from the Ministry of Health, Labour and Welfare of Japan.

Supplementary data

Supplementary data associated with this article can be found, in the online version, at http://dx.doi.org/10.1016/j.jhep.2012.01.027.

References

[1] Malhi H, Gores G. Cellular and molecular mechanisms of liver injury. Gastroenterology 2008;134:1641–1654.
[2] Hiramatsu N, Hayashi N, Katayama K, Mochizuki K, Kawanishi Y, Kasahara A, et al. Immunohistochemical detection of Fas antigen in liver tissue of patients with chronic hepatitis C. Hepatology 1994;19:1354–1359.
[3] Mochizuki K, Hayashi N, Hiramatsu N, Katayama K, Kawanishi Y, Kasahara A, et al. Fas antigen expression in liver tissues of patients with chronic hepatitis B. J Hepatol 1996;24:1–7.
[4] Feldstein A, Canbay A, Angulo P, Taniai M, Burgart L, Lindor K, et al. Hepatocyte apoptosis and fas expression are prominent features of human nonalcoholic steatohepatitis. Gastroenterology 2003;125:437–443.
[5] Kronenberger B, Wagner M, Herrmann E, Mihm U, Piiper A, Sarrazin C, et al. Apoptotic cytokeratin 18 neoepitopes in serum of patients with chronic hepatitis C. J Viral Hepat 2005;12:307–314.
[6] Papatheodoridis GV, Hadziyannis E, Tsochatzis E, Chrysanthos N, Georgiou A, Kafiri G, et al. Serum apoptotic caspase activity as a marker of severity in HBeAg-negative chronic hepatitis B virus infection. Gut 2008;57:500–506.
[7] Wieckowska A, Zein NN, Yerian LM, Lopez AR, McCullough AJ, Feldstein AE. In vivo assessment of liver cell apoptosis as a novel biomarker of disease severity in nonalcoholic fatty liver disease. Hepatology 2006;44:27–33.
[8] Moriya K, Fujie H, Shintani Y, Yotsuyanagi H, Tsutsumi T, Ishibashi K, et al. The core protein of hepatitis C virus induces hepatocellular carcinoma in transgenic mice. Nat Med 1998;4:1065–1067.
[9] Pikarsky E, Porat RM, Stein I, Abramovitch R, Amit S, Kasem S, et al. NF-kappaB functions as a tumour promoter in inflammation-associated cancer. Nature 2004;431:461–466.
[10] Takehara T, Tatsumi T, Suzuki T, Rucker Er, Hennighausen L, Jinushi M, et al. Hepatocyte-specific disruption of Bcl-xL leads to continuous hepatocyte apoptosis and liver fibrotic responses. Gastroenterology 2004;127:1189–1197.
[11] Hikita H, Takehara T, Shimizu S, Kodama T, Li W, Miyagi T, et al. Mcl-1 and Bcl-xL cooperatively maintain integrity of hepatocytes in developing and adult murine liver. Hepatology 2009;50:1217–1226.
[12] Weber A, Boger R, Vick B, Urbanik T, Haybaeck J, Zoller S, et al. Hepatocyte-specific deletion of the antiapoptotic protein myeloid cell leukemia-1 triggers proliferation and hepatocarcinogenesis in mice. Hepatology 2010;51:1226–1236.
[13] Fujise K, Zhang D, Liu J, Yeh ET. Regulation of apoptosis and cell cycle progression by MCL1. Differential role of proliferating cell nuclear antigen. J Biol Chem 2000;275:39458–39465.
[14] Jamil S, Sobouti R, Hojabrpour P, Raj M, Kast J, Duronio V. A proteolytic fragment of Mcl-1 exhibits nuclear localization and regulates cell growth by interaction with Cdk1. Biochem J 2005;387:659–667.
[15] Pawlikowska P, Leray I, de Laval B, Guihard S, Kumar R, Rosselli F, et al. ATM-dependent expression of IEX-1 controls nuclear accumulation of Mcl-1 and the DNA damage response. Cell Death Differ 2010;17:1739–1750.
[16] Jamil S, Mojtabavi S, Hojabrpour P, Cheah S, Duronio V. An essential role for MCL-1 in ATR-mediated CHK1 phosphorylation. Mol Biol Cell 2008;19:3212–3220.
[17] Takehara T, Hayashi N, Tatsumi T, Kanto T, Mita E, Sasaki Y, et al. Interleukin 1beta protects mice from Fas-mediated hepatocyte apoptosis and death. Gastroenterology 1999;117:661–668.
[18] Ito Y, Sasaki Y, Horimoto M, Wada S, Tanaka Y, Kasahara A, et al. Activation of mitogen-activated protein kinases/extracellular signal-regulated kinases in human hepatocellular carcinoma. Hepatology 1998;27:951–958.
[19] Chen F, Beezhold K, Castranova V. JNK1, a potential therapeutic target for hepatocellular carcinoma. Biochim Biophys Acta 2009;1796:242–251.
[20] Yan B, Wang H, Rabbani ZN, Zhao Y, Li W, Yuan Y, et al. Tumor necrosis factor-alpha is a potent endogenous mutagen that promotes cellular transformation. Cancer Res 2006;66:11565–11570.
[21] Lonkar P, Dedon PC. Reactive species and DNA damage in chronic inflammation: reconciling chemical mechanisms and biological fates. Int J Cancer 2011;128:1999–2009.
[22] Motoyama N, Wang F, Roth KA, Sawa H, Nakayama K, Negishi I, et al. Massive cell death of immature hematopoietic cells and neurons in Bcl-x-deficient mice. Science 1995;267:1506–1510.
[23] Rinkenberger JL, Horning S, Klocke B, Roth K, Korsmeyer SJ. Mcl-1 deficiency results in peri-implantation embryonic lethality. Genes Dev 2000;14:23–27.
[24] Willis SN, Chen L, Dewson G, Wei A, Naik E, Fletcher JI, et al. Proapoptotic Bak is sequestered by Mcl-1 and Bcl-xL, but not Bcl-2, until displaced by BH3-only proteins. Genes Dev 2005;19:1294–1305.
[25] Hikita H, Takehara T, Kodama T, Shimizu S, Hosui A, Miyagi T, et al. BH3-only protein bid participates in the Bcl-2 network in healthy liver cells. Hepatology 2009;50:1972–1980.
[26] Aravalli RN, Steer CJ, Cressman EN. Molecular mechanisms of hepatocellular carcinoma. Hepatology 2008;48:2047–2063.
[27] Kamata H, Honda S, Maeda S, Chang L, Hirata H, Karin M. Reactive oxygen species promote TNFalpha-induced death and sustained JNK activation by inhibiting MAP kinase phosphatases. Cell 2005;120:649–661.
[28] Schwabe RF, Brenner DA. Mechanisms of Liver Injury. I. TNF-alpha-induced liver injury: role of IKK, JNK, and ROS pathways. Am J Physiol Gastrointest Liver Physiol 2006;290:G583–G589.
[29] Bulua AC, Simon A, Maddipati R, Pelletier M, Park H, Kim KY, et al. Mitochondrial reactive oxygen species promote production of proinflammatory cytokines and are elevated in TNFR1-associated periodic syndrome (TRAPS). J Exp Med 2011;208:519–533.
[30] Nakahira K, Haspel JA, Rathinam VA, Lee SJ, Dolinay T, Lam HC, et al. Autophagy proteins regulate innate immune responses by inhibiting the release of mitochondrial DNA mediated by the NALP3 inflammasome. Nat Immunol 2011;12:222–230.
[31] Zhou R, Yazdi AS, Menu P, Tschopp J. A role for mitochondria in NLRP3 inflammasome activation. Nature 2011;469:221–225.
[32] Hanahan D, Weinberg RA. Hallmarks of cancer: the next generation. Cell 2011;144:646–674.
[33] Takehara T, Liu X, Fujimoto J, Friedman S, Takahashi H. Expression and role of Bcl-xL in human hepatocellular carcinomas. Hepatology 2001;34:55–61.
[34] Fleischer B, Schulze-Bergkamen H, Schuchmann M, Weber A, Biesterfeld S, Müller M, et al. Mcl-1 is an anti-apoptotic factor for human hepatocellular carcinoma. Int J Oncol 2006;28:25–32.
[35] Sieghart W, Losert D, Strommer S, Cejka D, Schmid K, Rasoul-Rockenschaub S, et al. Mcl-1 overexpression in hepatocellular carcinoma: a potential target for antisense therapy. J Hepatol 2006;44:151–157.
[36] Watanabe J, Kushihata F, Honda K, Sugita A, Tateishi N, Mominoki K, et al. Prognostic significance of Bcl-xL in human hepatocellular carcinoma. Surgery 2004;135:604–612.
[37] Hikita H, Takehara T, Shimizu S, Kodama T, Shigekawa M, Iwase K, et al. The Bcl-xL inhibitor, ABT-737, efficiently induces apoptosis and suppresses

growth of hepatoma cells in combination with sorafenib. Hepatology 2010;52:1310–1321.
[38] Chen CF, Lee WC, Yang HI, Chang HC, Jen CL, Iloeje UH, et al. Changes in serum levels of HBV DNA and alanine aminotransferase determine risk for hepatocellular carcinoma. Gastroenterology 2011;141:1240–1248.
[39] Bhala N, Angulo P, van der Poorten D, Lee E, Hui JM, Saracco G, et al. The natural history of nonalcoholic fatty liver disease with advanced fibrosis or cirrhosis: an international collaborative study. Hepatology 2011;54:1208–1216.
[40] Ruhl CE, Everhart JE. Elevated serum alanine aminotransferase and gamma-glutamyltransferase and mortality in the United States population. Gastroenterology 2009;136:477–485, e411.
[41] Pockros P, Schiff E, Shiffman M, McHutchison J, Gish R, Afdhal N, et al. Oral IDN-6556, an antiapoptotic caspase inhibitor, may lower aminotransferase activity in patients with chronic hepatitis C. Hepatology 2007;46:324–329.

SCIENTIFIC REPORTS

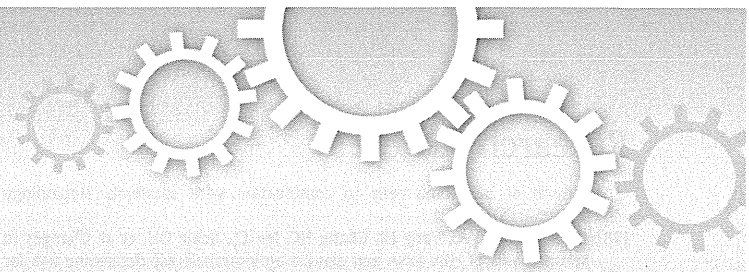

SUBJECT AREAS:
EXPRESSION SYSTEMS
BIOLOGICAL TECHNIQUES
GENE DELIVERY
GENE THERAPY

Received
17 November 2012

Accepted
27 December 2012

Published
25 January 2013

Correspondence and requests for materials should be addressed to Y.K. (kanegae@ims.u-tokyo.ac.jp)

* Current address: Japan Animal Referral Medical Center, 2-5-8 Kuji, Takatsu-ku, Kawasaki-shi, Kanagawa 213-0032, Japan.

Efficient production of adenovirus vector lacking genes of virus-associated RNAs that disturb cellular RNAi machinery

Aya Maekawa, Zheng Pei, Mariko Suzuki, Hiromitsu Fukuda*, Yohei Ono, Saki Kondo, Izumu Saito & Yumi Kanegae

Laboratory of Molecular Genetics, Institute of Medical Science, University of Tokyo, Minato-ku, Tokyo, Japan.

First-generation adenovirus vectors (FG AdVs) are widely used in basic studies and gene therapy. However, virus-associated (VA) RNAs that act as small-interference RNAs are indeed transcribed from the vector genome. These VA RNAs can trigger the innate immune response. Moreover, VA RNAs are processed to functional viral miRNAs and disturb the expressions of numerous cellular genes. Therefore, VA-deleted AdVs lacking VA RNA genes would be advantageous for basic studies, both *in vitro* and *in vivo*. Here, we describe an efficient method of producing VA-deleted AdVs. First, a VA RNA-substituted "pre-vector" lacking the original VA RNA genes but alternatively possessing an intact VA RNA region flanked by a pair of FRTs was constructed. VA-deleted AdVs were efficiently obtained by infecting 293hde12 cells, which highly express FLP, with the pre-vector. The resulting transduction titers of VA-deleted AdVs were sufficient for practical use. Therefore, VA-deleted AdVs may be substitute for current FG AdV.

E1- and E3-deleted adenovirus vectors (AdVs) developed in the middle of 1990's[1,2] are commonly known as first-generation (FG) AdVs, and have been extensively used not only for the basic studies of various gene functions *in vitro* and *in vivo* but also for preclinical and clinical gene therapy. Because FG AdVs lack E1A gene, which is an essential transactivator in all other viral promoters driven by RNA polymerase II. Therefore, FG AdVs were usually considered that they do not express any viral gene products. However, FG AdVs, in fact, express VA RNAs that are transcribed by RNA polymerase III when using these vectors both *in vitro* and *in vivo*, because its activity is probably independent of RNA polymerase II.

VA RNAs, VAI and VAII, located at about 30 map units on adenovirus 5 (Ad5), are non-coding RNAs consisting of 157–160 nucleotides (nt). These VA RNAs are extremely abundant during the late phase of infection and inhibit cellular RNA-interference pathways by saturating Exportin 5 and Dicer[3]. Also, VAI inhibits protein kinase R (PKR) activity and, consequently, eliminates the block of the cellular translation machinery to allow the efficient production of viral proteins. Moreover, VA RNAs were processed and generate miRNAs[4,5], known as mivaRNAI and mivaRNAII that disturb the expression of many cellular genes, with the probable result of blocking cellular antiviral machinery. Therefore, there is no doubt that the AdVs lacking VA RNA genes are superior to current FG AdVs.

VAI and VAII are also transcribed not only during the early phase of Ad5 but also in E1A-deleted FG AdV. An E1-containing Ad5 mutant virus is reported which lack the expressions of both VAI and VAII and can proliferate in human cells, but its titers are approximately 60-fold lower than that of wild-type Ad5[6]. Therefore, VA RNAs are not essential, but play an important role in efficient viral growth by overcoming cellular antiviral machinery. Although the E1-containing mutant virus lacking expression of VA RNAs can slightly grow, efficient systems for producing E1-, E3- and VA-deleted AdVs (simply denoted VA-deleted AdVs) are extremely difficult to develop. One system for generating VA-deleted AdV expressing GFP using a 293 cell line that inducibly expresses the VAI gene has been reported[7]. However, the transduction titer produced using this system is approximately 1,000-fold lower than that of current FG AdVs. Furthermore, 18 days (including a secondary passage) are required before VA-deleted AdV are first observed, and the aid of expression markers, such as GFP or luciferase fluorescence, may be necessary to isolate the VA-deleted AdV. Therefore, this production system using a VA-expressing cell line is impractical for general use.

We hypothesized that, although VA RNAs are not essential for viral growth, VA-deleted AdV cannot grow during the initial step of vector generation, where only a few copies of the viral genome are present per cell, possibly because viral genes other than VA RNAs that block the cellular antiviral machinery may not be

sufficiently expressed. The amount of VA RNAs expressed from the chromosomes of the established cell lines may be insufficient, probably because abundant VA RNAs are necessary in the late phase of viral replication. Therefore, we adopted a strategy in which a VA-containing FG AdV (denoted pre-vector) is extensively amplified using 293 cells and the pre-vector is then converted to VA-deleted AdV through the removal of the VA genes using recombinase-expressing 293 cells to obtain a large amount of VA-deleted AdVs sufficient for the simultaneous introduction of numerous viral copies to the cells. However, this strategy appeared unrealizable because it requires the 293 cell line highly expressing the recombinase sufficient to remove VA RNA genes completely from rapidly replicating pre-vector genomes. We have established the 293 cell line, 293hde12[8], that contains the codon-humanized FLPe (hFLPe) that highly expresses thermo-stable FLPe recombinase[9]. We here showed that the VA genes present in the pre-vector genome were virtually completely removed using this cell line and high-titer VA-deleted AdVs were efficiently obtained.

Results

Efficient production of VA-deleted AdVs. We first constructed a VA-expressing DNA fragment, FVF, that contains intact VAI and VAII genes (Fig. 1a) flanked with a couple of FRTs (F refers to FRT in this study). The splicing acceptor site present between the initiation codon of the terminal protein precursor (pTP) and the 5′ end of VAI was disrupted by replacing T with C to prevent possible aberrant splicing. Then, we constructed two structurally different EF-AdV pre-vectors expressing GFP under the control of the EF1α promoter, AxdV-4FVF-GFP and AxdV-FVF-GFP, in which the original VAI and VAII genes were disrupted and, instead, the functional FVF fragment was inserted at different positions. The former pre-vector lacks both B-box sequences of the VAI and VAII that are essential for the activity of the internal polymerase-III promoter because of the deletions of 15 nt and 17 nt, respectively, (Fig. 1b), and instead bears the FVF fragment at the E4 insertion site near the right end of the viral genome[10] (Fig. 1a, upper left). The latter pre-vector lacks most of the VAI and VAII regions because of a deletion of 381 nt (Fig. 1c) and contains the FVF fragment within this region (Fig. 2a, lower left). Both pre-vectors grew well in the 293 cells, and their transduction titers were only slightly lower than that of the control FG AdV (Table 1, 37×10^7 and 60×10^7 versus 83×10^7 copies/mL).

Then, 293hde12 cells that constitutively and highly express codon-humanized FLPe recombinase[8,11] were infected with pre-vectors to obtain the first stock of VA-deleted AdV. The vector lacking VA RNA genes grew efficiently in the 293hde12 cells, similar to the pre-vector genome in 293 cells, because the VA RNAs were supplied from the excised circular DNAs consisting of VA RNA genes and one copy of FRT (Fig. 2a, middle) and from the pre-vector genome prior to the FLP-mediated excision. Then, five times more volume of the first stock than usual was used to infect the 293hde12 cells to create the second stock. The vector replicated in the 293hde12 cells, probably because a large amount of VA-deleted AdV were infected: the titer of the vector in the first stock was very high, and a much larger volume of stock was used for infection. The resulting vectors were named AxdV-4F-GFP and AxdV-F-GFP, respectively (Fig. 2a, upper and lower right). When the vectors in the second stock were used to infect 293hde12 cells, a minimal degree of replications was observed. Using a high multiplicity of infection (MOI), however, the slight replication was observed though the replication progressed slowly. Vectors from the second stock were used for further characterization.

The transduction titers of VA-deleted AdVs were sufficient for practical use. Because VA-deleted AdV is difficult to grow in 293 cells, the conventional titration method for measuring viral growth cannot be used. Therefore, the transduction titers[12] of the VA-deleted AdV and the pre-vector were measured; these titers show the copy number of viral genomes successfully transduced into infected target cells as evaluated using real-time PCR. The titers of VA-deleted AdV, pre-vector, and commonly used FG AdV can be compared using this method. The transduction titers of both AxdV-4F-GFP and AxdV-F-GFP were only one order lower than those of their pre-vectors (14% and 12%, respectively, Table 1), indicating that the titers of the VA-deleted vectors were sufficient for practical use as an alternative to FG AdVs. Moreover, using the same strategy, we produced other VA-deleted AdVs, such as AxdV-4F-NCre expressing Cre recombinase under the control of EF1α promoter and AxdV-F-SRChe expressing the Cherry marker under the control of the SRα promoter, and the resulting transduction titers were similar to those for AxdV-4F-GFP and AxdV-F-GFP (Table 1). Of note, the titer of Cre-expressing VA-deleted AdV was successfully obtained without trouble and was also quantitatively sufficient for general use, since Cre-expressing FG AdVs often exhibit a low titer and vector expansion is sometimes difficult.

Viral stocks of VA-deleted AdV likely contain a small amount of pre-virus that escaped the removal of the FVF fragment. Hence, HuH-7 cells were infected with AxdV-F-GFP and three days later, the transduced AdV DNA was examined using a Southern blot technique (Fig. 2b). The pre-vector DNA (2.7 kb) containing the VA genes clearly shifted to VA-deleted AdV DNA (2.2 kb), and no 2.7-kb band was detected in this assay. The result indicates that the VA RNAs in the pre-vector were efficiently removed during the replication of the pre-vector genome in 293hde12 cells. The same results were obtained when AxdV-4F-GFP was used (data not shown). The copy numbers of these viral genomes were examined using quantitative real-time PCR (qPCR) and VAI- and VAII-specific probes (Fig. 1a). Although the secondary structures of VAI and VAII are very similar, these probes were highly specific for one to the other (Supplementary Fig. S1). The pre-vector genome was present at approximately 1/90 or less, indicating that the purity of the VA-deleted AdV was about 99% or more.

Almost complete removal of contaminated pre-vector. To examine the level of VA RNAs expressed from contaminated pre-vector, the total cellular RNA of HuH-7 cells infected with AxdV-F-GFP was extracted and the expressed VA RNAs were analyzed using a northern blot technique (Fig. 2c). Neither VAI nor VAII were detected. In contrast, the pre-vector AxdV-FVF-GFP expressed considerable amounts of VAI and VAII. The same results were obtained when AxdV-4F-GFP was used (data not shown). The FG AdV AxCAGFP expressing GFP under control of CAG promoter does express similar amount of VA RNAs (data not shown). Expressed VAI and VAII RNA in cells infected with AxdV-4F-GFP or AxdV-F-GFP were also examined using qPCR after reverse transcription (Table 2). Both VAI and VAII were hardly detected, compared with the pre-vector infected in parallel, especially when using AxdV-4F-GFP, though 1% to 3% of the VA RNAs were detected when infected with AxdV-F-GFP. The Table 2 also showed that AxdV-4F-GFP and AxdV-F-GFP preparations expressed VA RNAI only about 1/300 and 1/120 less than FG AdV (0.02/5.97 and 0.05/5.97), respectively. These results correlated well with those of the Southern blot and qPCR analyses described above. Because contamination by the pre-vector of AxdV-4F-GFP was hardly detected using qPCR, an extremely sensitive bioassay was performed; 293 cells were infected with the VA-deleted AdV stock and the possible presences of pre-vector genome and VA RNAs expressed from the pre-vector were examined using Southern and northern blot techniques, respectively. Only the pre-vector genome must replicate efficiently in 293 cells. The amplified pre-vector genome was still not detected in a Southern blot analysis (Fig. 3a),

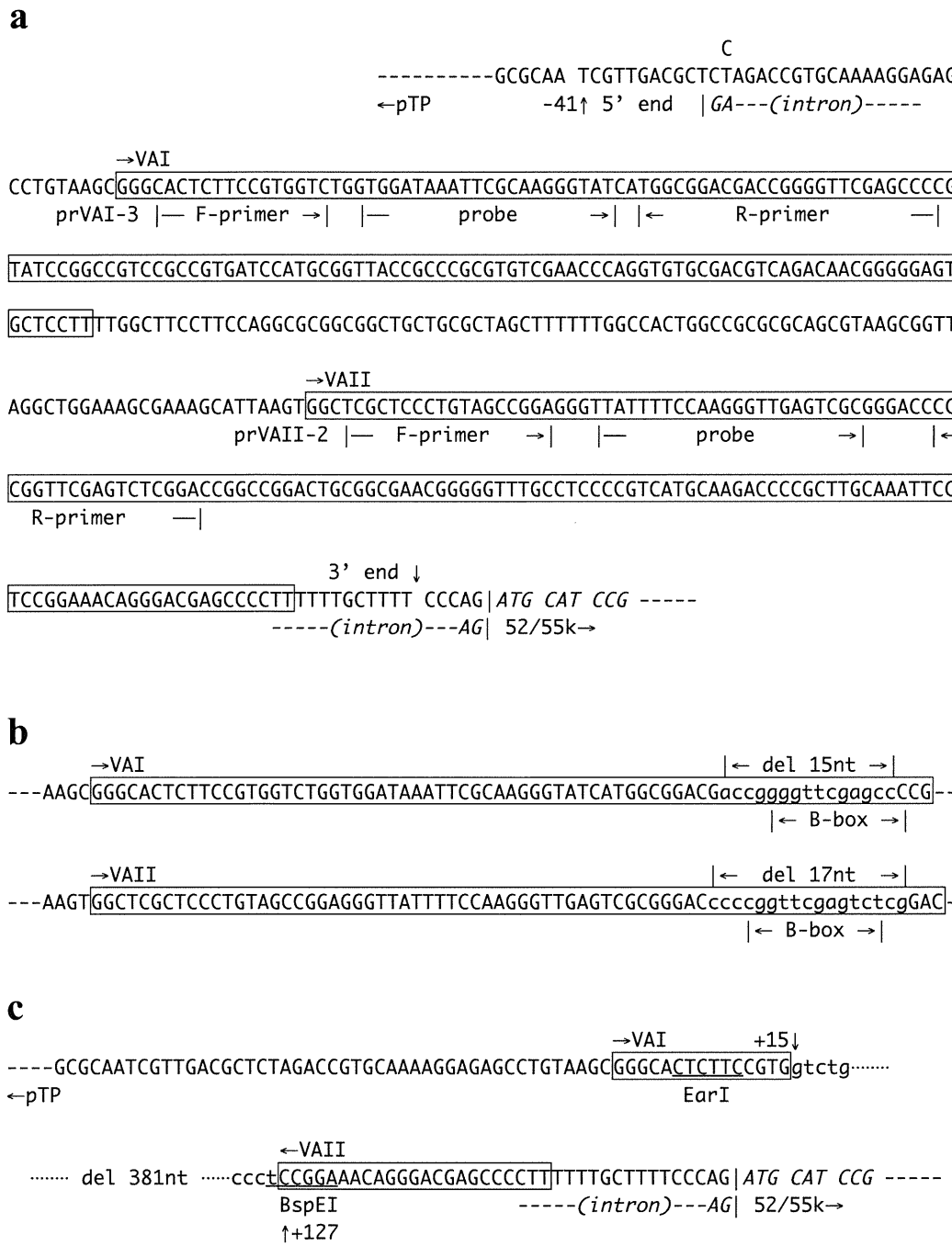

Figure 1 | Nucleotide sequences for VAI-VAII region. (a) VAI and VAII genes in the FVF fragment. VAI and VAII are boxed. prVAI-3 and prVAII-2 are the primers used for qPCR for the detection and quantification of VAI and VAII, respectively. Note that the actual R-primers are complementary to the sequences shown in this figure. pTP, terminal protein precursor; 52/55 k, 52 k and 55 k proteins. (b) B-box deletions of internal promoter in AxdV-4FVF-GFP and AxdV-4F-GFP. The deleted nucleotides are shown in small letters. (c) VAI-VAII deletion in AxdV-FVF-GFP and AxdV-F-GFP. The deleted region is shown in small letters. The deletion of 381 nt starts at 15 nt and 127 nt downstream from the 5′ end of VAI and VAII, respectively.

whereas the VA RNAs were slightly detected using a northern blot technique (Fig. 3b). Although the experiments using 293 cells were not quantitative, these results suggested that the amount of VA RNAs expressed from contaminated pre-vector in target cells other than 293 cells was minimal when the second stock was used. These results indicated that the VA-deleted AdVs produced using this production system were almost pure and may be used without consideration of the effect of VA RNAs in most studies. The contaminated circular DNA containing the VA-RNA genes was completely removed by purification of the vector.

To examine whether the VA-deleted AdV expresses a gene product as efficiently as FG AdV, HeLa cells were infected with VA-deleted AdVs and pre-vectors expressing GFP at the same transduction unit value and the resulting fluorescence was measured (Table 3). The VA-deleted AdVs showed similar expression levels to those of their pre-vectors.

Discussion

The efficient removal of VA RNA genes from the pre-virus genomes is crucial for this strategy. We here showed that 293hde12 cell line

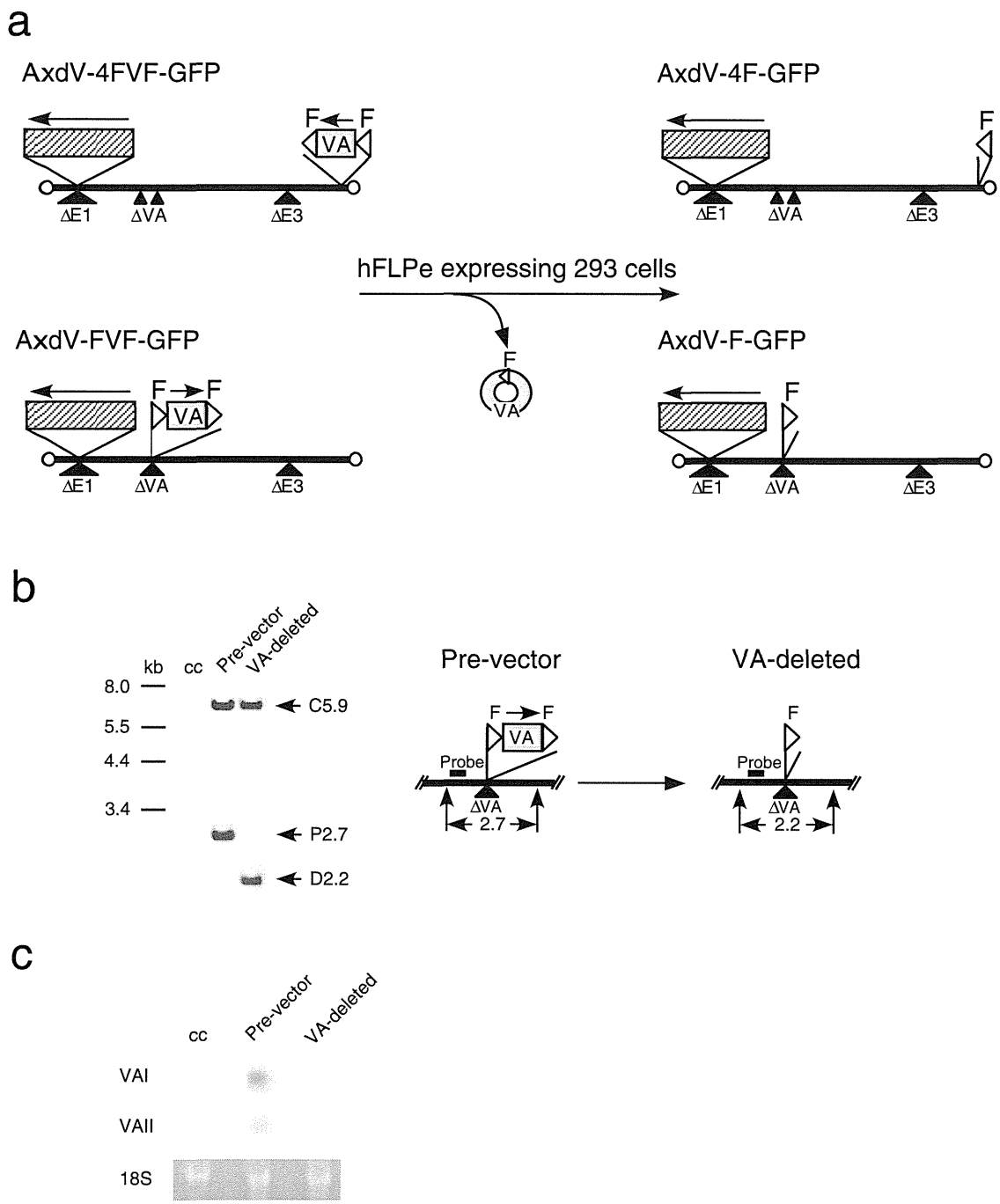

Figure 2 | Structures of pre-vectors and VA-deleted AdVs. (a) Strategy for the generation of VA-deleted vectors. F, FRT. Hatched box, GFP expression unit including EF1α promoter. An arrow shows the orientation of the transcription. (b) Removal of FVF fragment from the pre-vector AxdV-FVF-GFP genome. Total DNAs of infected HuH-7 cells were digested with *Kpn*I, and the DNA fragment containing FVF and F was detected using a Southern blot technique using the probe shown in the figure (enzyme, positions). C5.9 refers to the 5.9-kb fragment derived from outside of this region (1.7-kb *Bgl*II fragment, nt 30823-82495), showing that the amounts of the vector genomes were almost the same. cc, uninfected control cells; P, pre-vector; D, VA-deleted AdV. (c) Detection of expressed VA RNAs. Total RNAs of the same infected HuH-7 cells were analyzed using a northern blot technique. 18 S, 18 S ribosomal RNA.

that highly and constitutively express FLP recombinase was sufficient for this purpose. The cell lines constitutively expressing Cre have been used for production of helper-dependent AdVs, which contain a large DNA up to about 30kb. The viral packaging region of the helper virus must be excised out from the replicating viral genome but the excision efficiency is less than that described here[13,14] and hence the contaminated helper virus must be removed by the buoyant centrifugation using cesium chloride. Probably such incomplete excision might result from the toxicity of highly expressed Cre in 293 cells[15–18], while no toxicity of FLP has so far been reported. Therefore, 293hde12 cells played the most important role in this production system.

Furthermore, we demonstrated in this work that the AdVs containing two FRT sequences at the VA RNA region in the viral

Table 1 | Transduction titers of VA-deleted AdVs

AdV	Type	Transduction titer copies/mL ($\times 10^7$)	Ratio (%)
AxdV-4FVF-GFP	pre-vector	37	100
AxdV-4F-GFP	VA-deleted	5	14
AxdV-FVF-GFP	pre-vector	60	100
AxdV-F-GFP	VA-deleted	7	12
AxdV-4FVF-NCre	pre-vector	47	100
AxdV-4F-NCre	VA-deleted	4	8
AxdV-FVF-SRChe	pre-vector	20	100
AxdV-F-SRChe	VA-deleted	2	12

The transduction titer of the control FG AdV, AxEFGFP, was 83×10^7 copies/mL. The transduction titer was called the relative vector titer (rVT)[12], which is about five-times lower than the conventional $TCID_{50}$ titer of the pre-virus measured using 293 cells (see Methods).

genome, AxdV-F-GFP etc., were viable and their titers were comparable to FG AdV. When a foreign DNA sequence is inserted into the AdV genome, even when the sequence is short such as recombination targets, the AdVs are often not viable or their titers are very low, probably because the small insertion influences on the replication of the AdV genome. For this reason only three positions, i.e. as the substitutions of E1 and E3 genes and the insertion upstream of E4 genes, are generally used. Hence, we first constructed AxdV-4F-GFP because we knew that the AdVs containing foreign DNA at the E4 insertion position was very stable shown by our early works[1,19]. Then, we tried the original site of VA RNA genes and demonstrated that the FRTs can successfully be inserted at the VA RNA region causing only slight reduction of the AdV titers.

This production system described here may allow the practical application of VA-deleted AdVs as a possible alternative to current FG AdVs, since the transduction titer was only one order lower than that of FG AdVs and, in fact, we have already produced more than twenty VA-deleted AdVs expressing various genes without any difficulty. Because VA RNAs may disturb experimental results that are obtained using FG AdVs to some extent, VA-deleted AdVs are likely to be preferable for many types of basic research using adenovirus vectors. When examining the influences of VA RNAs on previously obtained results, the pre-vector can be used as an ideal control for VA-deleted AdVs. Although the target genes of VA RNAs are not clear at present, Aparicio *et al.*[5] reported that the expressions of many genes including TIA-1, a splicing and translation regulator, are down-regulated by mivaRNAs, which are the processed products of VA RNAs, and they proposed that TIA-1 may be one such target of mivaRNAs. We compared the expression of TIA-1 using a VA-deleted AdV and its pre-vector and observed that TIA-1 expression was slightly downregulated but was not statistically significant in our assay system. Because they did not use a VA-deleted vector but rather E1-containing viruses that efficiently replicate in infected cells and probably express much more VA RNAs. Therefore, their results are not necessarily contradictory and may be explained by the quantitative differences of expressed VA RNAs. We found other genes that were downregulated by VA RNAs (YK, unpublished results). Studies on the influences of VA RNAs on immune responses *in vivo* are also underway. So far, we found that the immune response caused by VA RNA was lower than that by aberrantly expressed viral pIX protein[20] but quantitative analyses are needed to clarify this issue. Notably, VA-deleted AdVs are probably superior to the current FG AdV for researches involving AdVs expressing siRNA and miRNA, since VA RNAs expressed by FG AdVs may compete with them and disturb the effects of these RNAs[3]. In fact, an shRNA expressed using VA-deleted AdV was more effective than that using current FG AdV (manuscript in preparation). These small-RNA technologies are extensively used in various research fields including signal transduction, cell differentiation and iPS study. Because more than three hundred papers have been published so far using FG AdVs expressing siRNA or miRNA based on our PubMed searching, VA-deleted AdV may be valuable in these fields.

The production level may be sufficient to apply VA-deleted AdVs to gene therapy as a safer alternative to existing practices. To what extent VA-deleted AdVs reduce immune responses in gene therapy of humans remain to be elucidated. Another possible contribution to gene therapy using AdVs is that, VA-deleted AdVs may considerably reduce contamination with replication-competent AdVs (RCA), one of the problems in the production of gene-therapy grade AdVs, because even if VA-deleted RCA is generated, only very low levels of replication would occur in human cells. Moreover, as proposed by Carnero *et al.*[4], a VA-deleted replication-competent adenovirus produced using this method could be used as an oncolytic virus that specifically replicate in cells with inactive PKR, such as tumor cells with activated ras or Epstein-Barr virus.

The same strategy described here could also be applied to studies of other DNA viruses, such as herpes viruses, because drug-resistant cell lines that highly express viral genes essential for the viral life cycle are often difficult to obtain because of their slight toxicity to cell growth. Moreover, using this strategy and recombinase-expressing cells, two or more genes could be deleted simultaneously using mutant *lox*P 2272[21] and FRT mutants[22,23] that exclusively recombine two identical mutant recombinase-targets. In conclusion, this strategy may accelerate studies using adenovirus vectors and may contribute to gene therapy.

Methods

Cells and virus titration. Human cell lines of 293[24], HeLa and HuH-7 are derived from the embryonic kidney, the cervical carcinoma and the hepatocellular carcinoma, respectively. These cells were cultured in DMEM supplemented with 10% fetal calf serum (FCS). The 293 cells constitutively express adenoviral E1 genes and support the replication of E1-substituted AdVs. 293hde12 is a 293 cell line possessing the hFLPe gene[8], an improved version of the FLPe gene[9], in which the codon usage has been changed to that used in humans and which produces more FLPe enzyme. 293hde12 cells were cultured in DMEM supplemented with 10% FCS plus geneticin (0.75 mg/mL). After infection with AdVs, the cells were maintained in DMEM supplemented with 5% FCS without geneticin.

All the AdVs were titrated using the method of transduction titer known as the relative vector titer (copies/mL)[12]. In this titration method, the copy number of viral genomes successfully transduced into the infected target cells, such as HeLa or HuH-7 cells, are measured using real-time PCR. The transduction titer method can be used not only for VA-deleted AdV, but also for FG AdVs, including the pre-vectors. This method enabled us to compare the various titers, since the transduction titer is not influenced by the growth rate of 293 cells, even if an expressed gene product (such as Cre or dsRed) is slightly deleterious to 293 cells[12]. When the gene product is not deleterious, the titer obtained using this method corresponds to about one fifth of that using either a 50% tissue culture infectious dose ($TCID_{50}$/mL)[25,26] or a plaque assay; the reason for this difference is probably because the transduction efficiency of 293 cells is much higher than that of other cells. The sequences of TaqMan probes for the titration (named AdV-1[10,12]) are derived from Ad5 pIX gene: forward primer, 5′-TGTGATGGGCTCCAGCATT-3′; probe, 5′-ATGGTCGCCCCGTCCTGCC-3′; reverse primer, 5′-TCGTAGGTCAAGGTAGTAGAGTTTGC-3′. A recommended protocol of the titration is available as Supplementary data of reference 12.

Table 2 | Expression levels of VAI and VAII RNAs measured using qPCR

		VA RNAs			
		I		II	
AdVs	Type	Copies $\times 10^8$	Ratio (%)	Copies $\times 10^8$	Ratio (%)
AxdV-4FVF-GFP	pre-vector	4.47 ± 0.81	100	1.36 ± 0.15	100
AxdV-4F-GFP	VA-deleted	0.02 ± 0.00	<1	ND	<1
AxdV-FVF–GFP	pre-vector	1.81 ± 0.06	100	1.83 ± 0.32	100
AxdV-F-GFP	VA-deleted	0.05 ± 0.00	2.9	0.03 ± 0.00	1.4
AxCAGFP	control FG AdV	5.97 ± 0.83		4.17 ± 0.16	

HuH-7 cells were infected with 50 μL of conventional stock of the pre-vector and the second stock of VA-deleted AdV. The method for preparation of the second stock is described in the Method section.

Plasmids. The pVA41da plasmid contains a DNA fragment covering the entire VAI and VAII from nt position 10576–11034 (Fig. 1a) of adenovirus type 5. A splicing acceptor site upstream of the pTp gene was disrupted, as described in the text. The region of functional VAI and VAII was excised as a *Hin*dIII-*Xba*I fragment and inserted at a *Swa*I site of pUFwF[27]; the resulting plasmid and DNA fragment containing intact VAI and VAII flanked two FRTs were named pUFVA41daF and FVF fragment, respectively.

Vector construction. All the AdVs described here were constructed using the cosmid cassette pAxcwit2 containing the full-length AdV genome[28]. The pre-vector cassette pAxdV-4FVF-w (w refers to the SwaI cloning site at the E1 region, see below) possesses the AdV genome in which VAI and VAII genes are disrupted by 15-nt and 17-nt deletions in their B-box sequences, respectively (Fig. 1b). The AdV genome contains the FVF fragment at the *Sna*BI site (nt position 35770) located in the E4 region at 165-nt downstream from the right end of the Ad5 genome[10]. A GFP-expressing unit under the control of the EF1α promoter[29] was inserted into the *Swa*I cloning site at the authentic E1 substitution region to obtain the pre-vector cosmid pAxdV-4FVF-GFP. The EF1α promoter in the left orientation was adopted to express the GFP because the use of the promoter in this manner greatly reduces the immune response of AdV, compared with the CAG and CMV promoters[20,30]. The pre-vector AxdV-4FVF-NCre and VA-deleted AdV AxdV-4F-NCre possess identical structures to AxdV-4FVF-GFP and AxdV-4F-GFP, respectively, except that the GFP gene is replaced by a Cre recombinase gene tagged with a nuclear localization signal[31]. The other pre-vector cosmid cassette pAxdV-FVF-4c lacks the VAI and VAII genes because of a large deletion from nt 10635 to nt 11012 and instead carries the FVF fragment. Note that this cassette contains two cloning sites, the *Swa*I site in the E1 region and the *Cla*I site in the E4 region (as described above), and is useful for the simultaneous expression of two genes. The pre-vector cosmid pAxdV-FVF-GFP was obtained by inserting the GFP expression unit described above at the *Swa*I site. Also, another pre-vector cosmid pAxdV-FVF-4Che contains the Cherry marker gene (Clontech) under the control of an SRα promoter[32] at this *Cla*I site. Then, the pre-vector AxdV-FVF-GFP, the VA-deleted vector AxdV-F-GFP, the pre-vector AxdV-FVF-4SRChe, and the VA-deleted AdV, AxdV-F-4SRChe were obtained using these pre-vector cosmid cassettes. The procedure to produce VA-deleted AdVs was as follows: the pre-vector genome in the cosmid cassette described above was excised with *Pac*I and transfected into 293 cells. The obtained pre-vector was then amplified twice using 293 cells and was used to infect 293hde12 cells at 10 copies/cell of transduction multiplicity of infection (MOI) to obtain VA-deleted AdVs. Then, This VA-deleted AdVs were used to infect 293hde12 cells at 10 copies/cell. The resultant viral stock is called the second stock in the Result section.

Quantitative Real-time PCR. The RNA expressions of VAI and VAII were quantified using the primers and probes described in Fig. 1a. The sequences of the GFP primers were as follows:
forward primer, CTACAACAGCCACAACGTCTATATCA;
probe, CGACAAGCAGAAGAACGGCATCAAGG;
reverse primer, ATGTTGTTGCGGATCTTGAAG.
The total RNA of the infected cells was extracted, and the amounts of the expressed

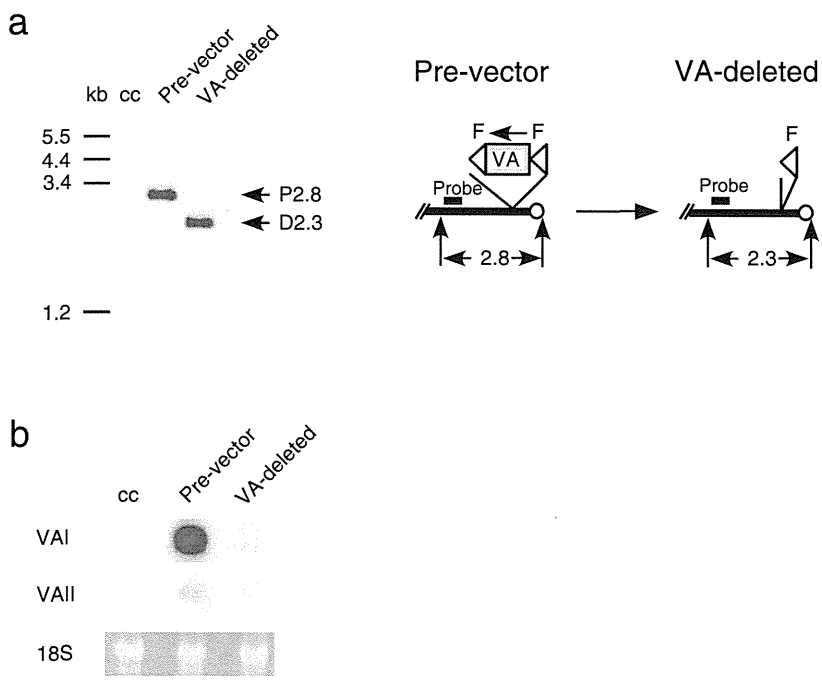

Figure 3 | Viral genome and expressed VA-RNA of contaminated pre-vector replicating in 293 cells. (a) Removal of the FVF fragment from the genome of the replicating pre-vector. Total DNAs of 293 cells infected with 15 μL of AxdV-4F-GFP stock were digested with *Eco*RV and the DNA fragment containing FVF and F was detected using a Southern blot technique. Other presentations are the same as in Fig. 1. (b) Detection of the expressed VA RNAs. Total RNAs of the same infected 293 cells were analyzed using a northern blot technique. 18 S, 18 S ribosomal RNA.

Table 3 | GFP expression in target cells infected with VA-deleted AdVs

AdV	Type	Ratio	
		fluorescence	expressed mRNA
AxdV-4FVF-GFP	pre-vector	1	1
AxdV-4F-GFP	VA-deleted	0.97 ± 0.15	0.81 ± 0.16
AxdV-FVF-GFP	pre-vector	1	1
AxdV-F-GFP	VA-deleted	1.14 ± 0.31	1.18 ± 0.20

HeLa cells were infected with pre-vector and VA-deleted AdV at a transduction MOI of 10. Three days later, GFP fluorescence was measured using a fluorometer and the GFP mRNA was quantified using reverse transcriptase and qPCR.

target RNA and 18S-rRNA (correction standard) were quantified using reverse-transcription and real-time PCR (Applied Biosystems Prism 7000); the ratio of the target RNA to 18S-rRNA was then calculated. The linear correlation between the amount of infected vector and the Ct values was confirmed (Supplementary Fig. S2). To quantify the DNA amount of VA RNAs and the AdV genome, the infected total cell DNA was prepared from cells using a previously described method[33,34] or a DNA preparation kit (Macherey-Nagel, through TaKaRa Bio). Quantitative PCR was performed to detect the AdV genome using a probe for the pIX gene described above[10,12]. The amount of chromosomal DNA was simultaneously measured to correct the Ct values of the viral genome per cell, and the corrected Ct was shown throughout. The probes were derived from the sequence of the human β-actin gene for HeLa and HuH7[10]. The qPCR reaction was performed according to the manufacturer's protocol: 50°C for 2 min and 95°C for 10 min, followed by 40 cycles of 95°C for 15 sec and 60°C for 1 min (Applied BioSystems).

Southern blotting analysis. HuH-7 cells in a 6-cm dish were infected with VA-deleted AdV and its pre-vector, and three days later the total DNA was prepared from the dish. Before alkaline treatment, the agarose gel was exposed to 0.1-N HCl for partial depurination, causing the DNA fragmentation of several hundred base pairs to obtain the complete transfer to the membrane[33]. The DNA was then transferred to the nylon membrane Hybond-N (Amersham GE) using the capillary-transfer method. Specific DNA was detected using a DIG DNA Labeling and Detection Kit (Roche Diagnostics). The probe DNA fragment derived from the viral genome was labeled with digoxigenin-UTP, and specific DNA was detected using the chemiluminescence of CDP-Star (Roche Diagnostics); the bands were visualized using LAS-4000 (Fuji Film).

Northern blotting analysis. The cells indicated in the figure legends were infected with pre-vector and VA-deleted AdV, respectively, at a transduction MOI of 10 copies/mL. The total RNA of the infected cells was extracted, and 30 μg per lane was electrophoresed in the agarose gel with tris-acetate-EDTA buffer. The RNA was transferred to the nylon membrane Hybond-N$^+$ (Amersham GE) using the capillary-transfer method. Specific RNA was detected using a DIGDNA Labeling and Detection Kit (Roche Diagnostics).

1. Miyake, S. *et al.* Efficient generation of recombinant adenoviruses using adenovirus DNA-terminal protein complex and a cosmid bearing the full-length virus genome. *Proc. Natl. Acad. Sci. U S A* **93**, 1320–1324 (1996).
2. Anton, M. & Graham, F. L. Site-specific recombination mediated by an adenovirus vector expressing the Cre recombinase protein: a molecular switch for control of gene expression. *J. Virol.* **69**, 4600–4606 (1995).
3. Lu, S. & Cullen, B. R. Adenovirus VA1 noncoding RNA can inhibit small interfering RNA and MicroRNA biogenesis. *J. Virol.* **78**, 12868–12876 (2004).
4. Carnero, E., Sutherland, J. D. & Fortes, P. Adenovirus and miRNAs. *Biochim. Biophys. Acta* **1809**, 660–667 (2011).
5. Aparicio, O. *et al.* Adenovirus VA RNA-derived miRNAs target cellular genes involved in cell growth, gene expression and DNA repair. *Nucleic Acids Res* **38**, 750–763 (2010).
6. Bhat, R. A., Domer, P. H. & Thimmappaya, B. Structural requirements of adenovirus VAI RNA for its translation enhancement function. *Mol. Cell Biol.* **5**, 187–196 (1985).
7. Machitani, M. *et al.* Development of an adenovirus vector lacking the expression of virus-associated RNAs. *J. Control Release* **154**, 285–289 (2011).
8. Takata, Y., Kondo, S., Goda, N., Kanegae, Y. & Saito, I. Comparison of efficiency between FLPe and Cre for recombinase-mediated cassette exchange in vitro and in adenovirus vector production. *Genes Cells* **16**, 765–777 (2011).
9. Buchholz, F., Angrand, P. O. & Stewart, A. F. Improved properties of FLP recombinase evolved by cycling mutagenesis. *Nat. Biotechnol.* **16**, 657–662 (1998).
10. Kanegae, Y. *et al.* High-level expression by tissue/cancer-specific promoter with strict specificity using a single-adenoviral vector. *Nucleic Acids Res.* **39**, e7 (2011).
11. Kondo, S., Takata, Y., Nakano, M., Saito, I. & Kanegae, Y. Activities of various FLP recombinases expressed by adenovirus vectors in mammalian cells. *J. Mol. Biol.* **390**, 221–230 (2009).
12. Pei, Z., Kondo, S., Kanegae, Y. & Saito, I. Copy number of adenoviral vector genome transduced into target cells can be measured using quantitative PCR: application to vector titration. *Biochem. Biophys. Res. Commun.* **417**, 945–950 (2012).
13. Ng, P., Evelegh, C., Cummings, D. & Graham, F. L. Cre levels limit packaging signal excision efficiency in the Cre/loxP helper-dependent adenoviral vector system. *J. Virol.* **76**, 4181–4189 (2002).
14. Ng, P., Parks, R. J. & Graham, F. L. Preparation of helper-dependent adenoviral vectors. *Methods Mol. Med.* **69**, 371–388 (2002).
15. Loonstra, A. *et al.* Growth inhibition and DNA damage induced by Cre recombinase in mammalian cells. *Proc. Natl. Acad. Sci. U S A* **98**, 9209–9214 (2001).
16. Pfeifer, A., Brandon, E. P., Kootstra, N., Gage, F. H. & Verma, I. M. Delivery of the Cre recombinase by a self-deleting lentiviral vector: efficient gene targeting in vivo. *Proc. Natl. Acad. Sci. U S A* **98**, 11450–11455 (2001).
17. Silver, D. P. & Livingston, D. M. Self-excising retroviral vectors encoding the Cre recombinase overcome Cre-mediated cellular toxicity. *Mol. Cell* **8**, 233–243 (2001).
18. Baba, Y., Nakano, M., Yamada, Y., Saito, I. & Kanegae, Y. Practical range of effective dose for Cre recombinase-expressing recombinant adenovirus without cell toxicity in mammalian cells. *Microbiol. Immunol.* **49**, 559–570 (2005).
19. Saito, I., Oya, Y., Yamamoto, K., Yuasa, T. & Shimojo, H. Construction of nondefective adenovirus type 5 bearing a 2.8-kilobase hepatitis B virus DNA near the right end of its genome. *J. Virol.* **54**, 711–719 (1985).
20. Nakai, M. *et al.* Expression of pIX gene induced by transgene promoter: possible cause of host immune response in first-generation adenoviral vectors. *Hum. Gene Ther.* **18**, 925–936 (2007).
21. Lee, G. & Saito, I. Role of nucleotide sequences of loxP spacer region in Cre-mediated recombination. *Gene* **216**, 55–65 (1998).
22. Schlake, T. & Bode, J. Use of mutated FLP recognition target (FRT) sites for the exchange of expression cassettes at defined chromosomal loci. *Biochemistry* **33**, 12746–12751 (1994).
23. Nakano, M., Ishimura, M., Chiba, J., Kanegae, Y. & Saito, I. DNA substrates influence the recombination efficiency mediated by FLP recombinase expressed in mammalian cells. *Microbiol. Immunol.* **45**, 657–665 (2001).
24. Graham, F. L., Smiley, J., Russell, W. C. & Nairn, R. Characteristics of a human cell line transformed by DNA from human adenovirus type 5. *J. Gen. Virol.* **36**, 59–74 (1977).
25. Precious, B. & Russell, W. C. Growth, purification and titration of adenoviruses. In *Virology: a practical approach.* (ed. Mahy, B. W. J.) 128–152 (IRL press, Oxford; 1991).
26. Kanegae, Y., Makimura, M. & Saito, I. A simple and efficient method for purification of infectious recombinant adenovirus. *Jpn J. Med. Sci. Biol.* **47**, 157–166 (1994).
27. Nakano, M. *et al.* Efficient gene activation in cultured mammalian cells mediated by FLP recombinase-expressing recombinant adenovirus. *Nucleic Acids Res.* **29**, E40 (2001).
28. Fukuda, H., Terashima, M., Koshikawa, M., Kanegae, Y. & Saito, I. Possible mechanism of adenovirus generation from a cloned viral genome tagged with nucleotides at its ends. *Microbiol. Immunol.* **50**, 643–654 (2006).
29. Kim, D. W., Uetsuki, T., Kaziro, Y., Yamaguchi, N. & Sugano, S. Use of the human elongation factor 1 alpha promoter as a versatile and efficient expression system. *Gene* **91**, 217–223 (1990).
30. Chiyo, T. *et al.* Conditional gene expression in hepatitis C virus transgenic mice without induction of severe liver injury using a non-inflammatory Cre-expressing adenovirus. *Virus Res.* **160**, 89–97 (2011).
31. Kanegae, Y. *et al.* Efficient gene activation in mammalian cells by using recombinant adenovirus expressing site-specific Cre recombinase. *Nucleic Acids Res.* **23**, 3816–3821 (1995).
32. Takebe, Y. *et al.* SR alpha promoter: an efficient and versatile mammalian cDNA expression system composed of the simian virus 40 early promoter and the R-U5 segment of human T-cell leukemia virus type 1 long terminal repeat. *Mol. Cell Biol.* **8**, 466–472 (1988).
33. Saito, I., Groves, R., Giulotto, E., Rolfe, M. & Stark, G. R. Evolution and stability of chromosomal DNA coamplified with the CAD gene. *Mol. Cell Biol.* **9**, 2445–2452 (1989).

34. Nakano, M. *et al.* Production of viral vectors using recombinase-mediated cassette exchange. *Nucleic Acids Res.* **33**, e76 (2005).

Acknowledgements

We thank Ms M. Terashima for excellent technical support and Ms E. Kondo for secretarial assistance. This work was supported in part by Grants-in-Aid from the Ministry of Education, Culture, Sports, Science and Technology to Y.K. and S.K. and the Ministry of Health, Labour and welfare ; by Research on the innovative development and the practical application of new drugs for hepatitis B to I.S.

Author contributions

A.M. performed the experiments and contributed to the writing of the manuscript. Z.P., M.S., H.F., Y.O. and S.K. performed the experiments. I.S. discussed the data and wrote the manuscript. Y.K. designed the strategies and performed the experiments. All the authors discussed the results and commented on the manuscript.

Additional information

Supplementary information accompanies this paper at http://www.nature.com/scientificreports

Competing financial interests: The authors declare no competing financial interests.

How to cite this article: Maekawa, A. *et al.* Efficient production of adenovirus vector lacking genes of virus-associated RNAs that disturb cellular RNAi machinery. *Sci. Rep.* **3**, 1136; DOI:10.1038/srep01136 (2013).

Virology 432 (2012) 29–38

Contents lists available at SciVerse ScienceDirect

Virology

journal homepage: www.elsevier.com/locate/yviro

Trans-complemented hepatitis C virus particles as a versatile tool for study of virus assembly and infection

Ryosuke Suzuki [a,*], Kenji Saito [a], Takanobu Kato [a], Masayuki Shirakura [b], Daisuke Akazawa [a], Koji Ishii [a], Hideki Aizaki [a], Yumi Kanegae [c], Yoshiharu Matsuura [d], Izumu Saito [c], Takaji Wakita [a], Tetsuro Suzuki [e,**]

[a] *Department of Virology II, National Institute of Infectious Diseases, 1-23-1 Toyama, Shinjuku-ku, Tokyo 162-8640, Japan*
[b] *Influenza Virus Research Center, National Institute of Infectious Diseases, Tokyo 208-0011, Japan*
[c] *Institute of Medical Science, University of Tokyo, Tokyo 108-8639, Japan*
[d] *Research Institute for Microbial Diseases, Osaka University, Osaka 565-0871, Japan*
[e] *Department of Infectious Diseases, Hamamatsu University School of Medicine, 1-20-1 Handayama, Higashi-ku, Hamamatsu, Shizuoka 431-3192, Japan*

ARTICLE INFO

Article history:
Received 30 March 2012
Returned to author for revisions
23 April 2012
Accepted 25 May 2012
Available online 22 June 2012

Keywords:
HCV
HCVtcp
Trans-packaging
Single-round infection

ABSTRACT

In this study, we compared the entry processes of *trans*-complemented hepatitis C virus particles (HCVtcp), cell culture-produced HCV (HCVcc) and HCV pseudoparticles (HCVpp). Anti-CD81 antibody reduced the entry of HCVtcp and HCVcc to almost background levels, and that of HCVpp by approximately 50%. Apolipoprotein E-dependent infection was observed with HCVtcp and HCVcc, but not with HCVpp, suggesting that the HCVtcp system is more relevant as a model of HCV infection than HCVpp. We improved the productivity of HCVtcp by introducing adapted mutations and by deleting sequences not required for replication from the subgenomic replicon construct. Furthermore, blind passage of the HCVtcp in packaging cells resulted in a novel mutation in the NS3 region, N1586D, which contributed to assembly of infectious virus. These results demonstrate that our plasmid-based system for efficient production of HCVtcp is beneficial for studying HCV life cycles, particularly in viral assembly and infection.

Introduction

Over 170 million people worldwide are chronically infected with hepatitis C virus (HCV), and are at risk of developing chronic liver diseases (Hoofnagle, 2002). HCV is an enveloped virus of the family *Flaviviridae*, and its genome is a positive-strand RNA consisting of the 5′-untranslated region (UTR), an open reading frame encoding viral proteins (core, E1, E2, p7, NS2, NS3, NS4A, NS4B, NS5A, and NS5B) and the 3′-UTR (Suzuki et al., 2007).

Host–virus interactions are required during the initial steps of viral infection. It was previously reported that CD81 (Bartosch et al., 2003a, b; McKeating et al., 2004; Pileri et al., 1998), scavenger receptor class B type I (Bartosch et al., 2003a, b; Scarselli et al., 2002), claudin-1 (Evans et al., 2007; Liu et al., 2009) and occludin (Benedicto et al., 2009; Evans et al., 2007; Liu et al., 2009; Ploss et al., 2009) are critical molecules for HCV entry into cells. CD81 interacts with HCV E2 via a second extracellular loop (Bartosch et al., 2003a, b; Hsu et al., 2003) and its role in the internalization process was confirmed (Cormier et al., 2004; Flint et al., 2006). It has also been shown that infectious HCV particles produced in cell cultures (HCVcc) exist as apolipoprotein E (ApoE)-enriched lipoprotein particles (Chang et al., 2007) and that ApoE is important for HCV infectivity (Owen et al., 2009).

Investigation of HCV had been hampered by difficulties in amplifying the virus in vitro before development of robust cell culture systems based on JFH-1 isolates (Lindenbach et al., 2005; Wakita et al., 2005; Zhong et al., 2005). Retrovirus-based HCV pseudoparticles (HCVpp), in which cell entry is dependent on HCV glycoproteins, have been used to study virus entry (Bartosch et al., 2003a; Hsu et al., 2003). Vesicular stomatitis virus (VSV)-based pseudotypic viruses bearing HCV E1 and E2 and replication-competent recombinant VSV encoding HCV envelopes have also been available as surrogate models for studies of HCV infection (Mazumdar et al., 2011; Tani et al., 2007).

It was recently shown that HCV subgenomic replicons can be packaged when structural proteins are supplied in *trans* (Adair et al., 2009; Ishii et al., 2008; Masaki et al., 2010; Steinmann et al., 2008). These *trans*-complemented HCV particles (HCVtcp) are infectious, but support only single-round infection and are unable to spread. Establishment of flexible systems to efficiently produce HCVtcp should contribute to studying HCV assembly, in particular encapsidation of the viral genome, and entry to cells with less stringent biosafety and biosecurity measures. Although single-round infection can be achieved by using the HCVcc system with receptor knock-out

* Corresponding author. Fax: +81 3 5285 1161.
** Corresponding author. Fax: +81 53 435 2338.
E-mail addresses: ryosuke@nih.go.jp (R. Suzuki), tesuzuki@hama-med.ac.jp (T. Suzuki).

0042-6822/$ - see front matter © 2012 Elsevier Inc. All rights reserved.
http://dx.doi.org/10.1016/j.virol.2012.05.033

cells, the single-round HCVcc system is not suitable for studying virus entry. We previously described plasmid-based production of HCVcc and HCVtcp (Masaki et al., 2010). Here, we demonstrated that HCVtcp production can be enhanced by introducing the previously reported cell-culture adaptive mutations and by deleting sequences not essential for replication in the subgenomic replicon construct. By providing genotype 1b-derived core-to-p7 in addition to intragenotypic viral proteins, chimeric HCVtcp were generated. Furthermore, blind passage of HCVtcp in the packaging cells resulted in the identification of a novel cell culture-adaptive mutation in NS3 that enables us to establish the efficient production of HCVtcp with structural proteins from various strains. Taken together, our system for producing single-cycle infectious HCV particles should be useful in the study of entry and assembly steps of the HCV life cycles. This technology may also have potential to be the basis for the safer vaccine development.

Results

Enhancement of HCVtcp production by adaptive mutations in E2, p7 and NS2 and by deleting sequences not essential for replication from replicon construct

In our HCVtcp system, the RNA polymerase I (Pol I)-driven replicon plasmid, which carries a dicistronic subgenomic luciferase reporter replicon of JFH-1 strain with a Pol I promoter and terminator (pHH/SGR-Luc), as well as a plasmid containing core-NS2 cDNA under the CAG promoter (pCAGC-NS2) were used (Masaki et al., 2010). In an effort to improve the yield of HCVtcp production, cell culture-adaptive mutations in E2 (N417S), p7 (N765D) and NS2 (Q1012R) which were previously selected from serial passage of HCVcc (Russell et al., 2008) were introduced into the core-NS2 expression plasmid (Fig. 1A) (residues are numbered

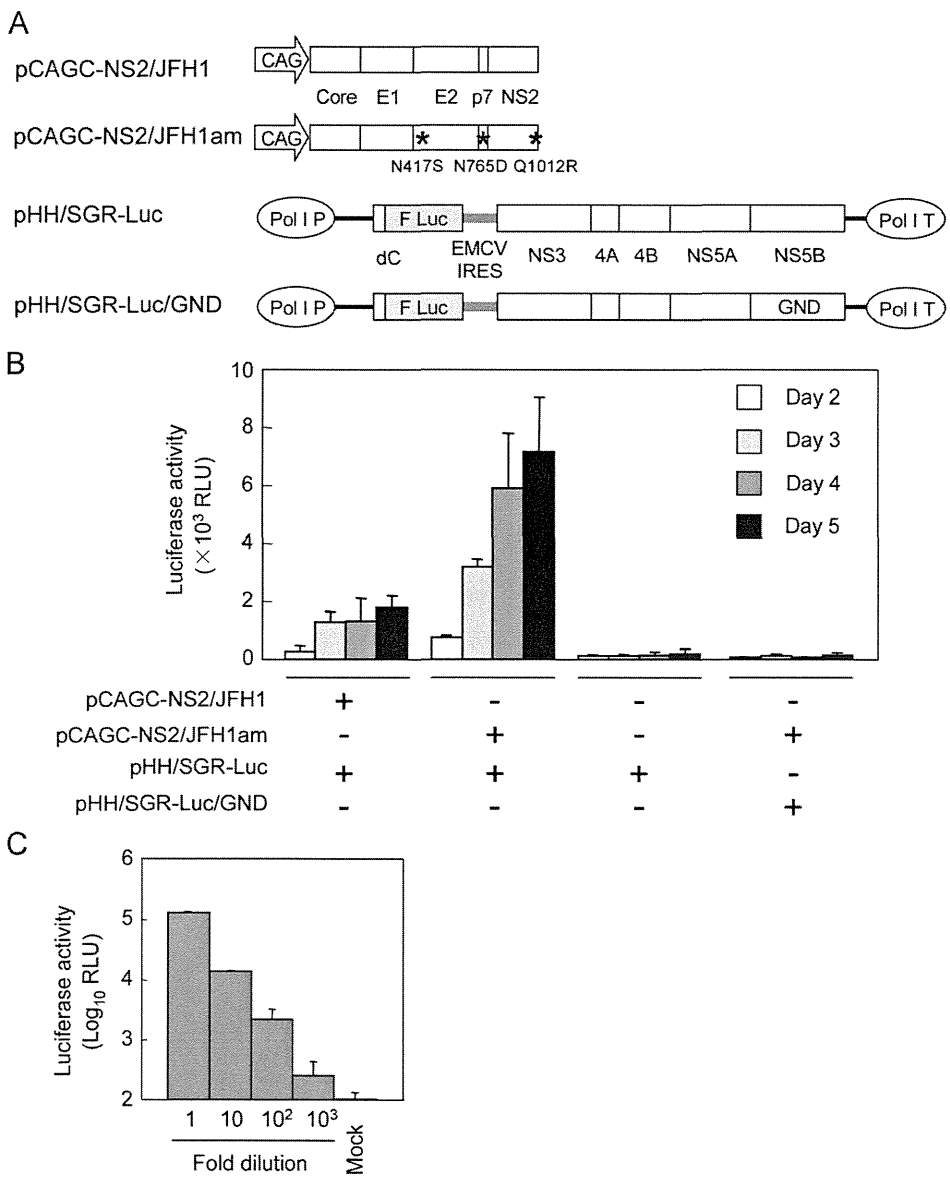

Fig. 1. HCVtcp production by two-plasmid transfection. (A) Schematic representation of plasmids is shown. HCV polyproteins derived from JFH-1 are indicated by white boxes. HCV UTRs are indicated by bold lines. The internal ribosomal entry site from encephalomyocarditis virus (EMCV IRES) is denoted as gray lines. Adaptive mutations are indicated as asterisks. F Luc: firefly luciferase gene; CAG: CAG promoter; Pol I P: RNA polymerase I promoter; Pol I T: RNA polymerase I terminator; GND: replication-deficient GND mutation. (B) Luciferase activity in Huh7.5.1 cells inoculated with supernatant from cells transfected with indicated plasmids at the indicated time points. Data are averages of triplicate values with error bars showing standard deviations. (C) Luciferase activity in cells inoculated with serially diluted HCVtcp.

according to positions within the JFH-1 polyprotein). Supernatants of cells transfected with plasmids (Fig. 1A) were collected and were used to infect Huh7.5.1 cells, which were analyzed by luciferase assay. Introduction of adaptive mutations (pCAGC-NS2/JFH1am) resulted in more than 4-fold higher production of HCVtcp at 5 day post-transfection, as compared to wild-type (WT) (pCAGC-NS2/JFH1) (Fig. 1B), indicating that the adaptive mutations contribute to enhancing HCVtcp production. To confirm that luciferase activity levels in HCVtcp-infected cells are correlated with the number of infectious particles, Huh7.5.1 cells were inoculated with serial dilutions of HCVtcp. Luciferase activity was well correlated with viral load (Fig. 1C), indicating that luciferase assay in HCVtcp-infected cells can be used to quantify HCV infection.

In order to further explore the efficient production of HCVtcp, we generated replicon constructs that lack the luciferase gene or include the partial coding sequences for structural proteins instead of reporter (Fig. 2A). Replication of each replicon in plasmid-transfected cells was then assessed by Western blotting (Fig. 2B). Among the constructs tested, NS5B levels were lowest in cells expressing pHH/SGR-Luc. NS5B levels in cells replicating other replicons appeared to be comparable. Cells were infected with supernatants of cells transfected with each replicon plasmid, along with pCAGC-NS2/JFH1am, followed by infectious unit assay (Fig. 2C). The highest production of HCVtcp was obtained from cells transfected with pHH/SGR, where the luciferase sequence was deleted from pHH/SGR-Luc, thus suggesting that deletion of the sequence not essential for RNA replication in the replicon may contribute to enhancing HCVtcp production.

Production of chimeric HCVtcp by providing heterologous core-p7

In order to elucidate whether *trans*-encapsidation of JFH-1 replicon can be achieved by providing core-p7 from other HCV strains, core-NS2 plasmids were constructed (Fig. 3A). In these plasmids, core through the N-terminal 33 aa of NS2, which contains transmembrane domain 1 of NS2, was derived from either H77c (genotype 1a), THpa (genotype 1b), Con1 (genotype 1b) or J6 (genotype 2a) strain. Residual NS2 was derived from JFH-1, as described previously (Pietschmann et al., 2006). HCVtcp was efficiently produced by core-p7 of J6 and THpa strains, but its production was less efficient in the case of Con1 strain. *Trans*-packaging was not detectable when core-p7 of H77c strain was used (Fig. 3C). Among HCV strains tested, difference in luciferase activity levels in HCVtcp-infected cells (Fig. 3C) were in agreement with that in the viral RNA levels in the culture supernatants of the transfected cells (Fig. 3B). Although the efficacy of *trans*-complementation was variable among strains, chimeric HCVtcp can be generated by providing genotype 1b-derived core-p7 in addition to intragenotypic viral proteins, and was used in subsequent studies.

ApoE- and CD81-dependent infection by HCVtcp

There is accumulating evidence that apolipoproteins, particularly ApoE, contribute to HCV production and infectivity (Chang et al., 2007; Owen et al., 2009). To determine whether ApoE is involved in infection of target cells by HCVtcp, we infected cells in the presence of increasing concentrations of anti-ApoE antibody.

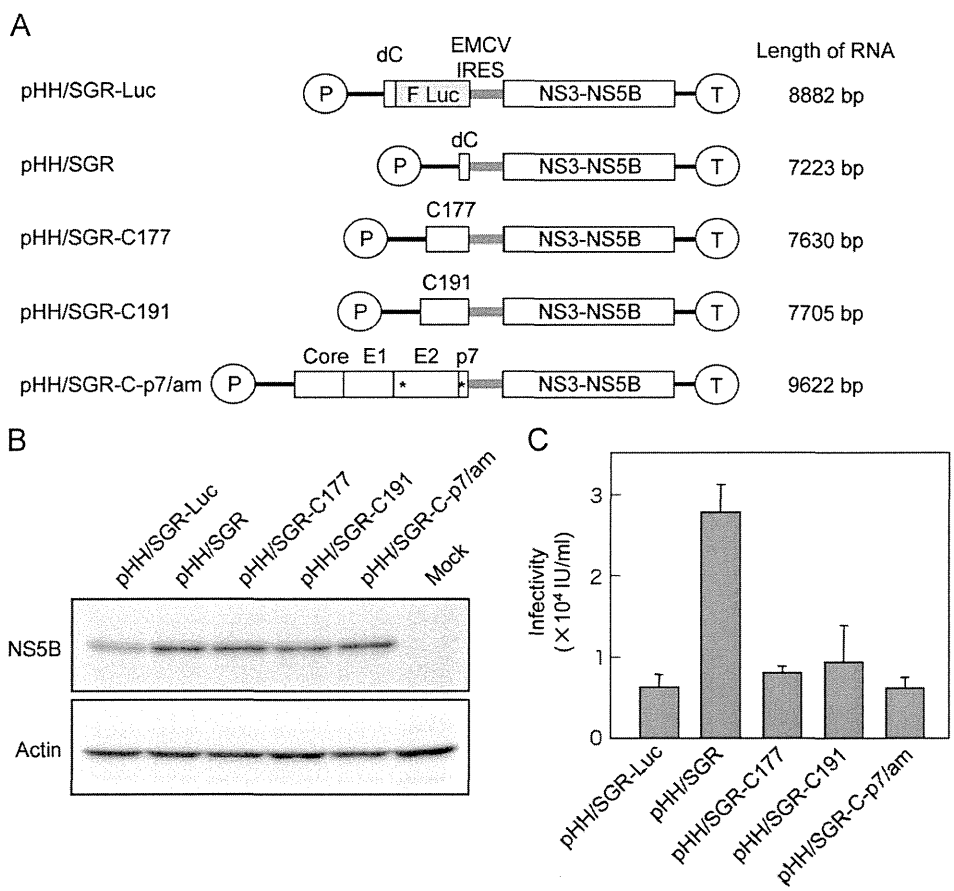

Fig. 2. Production of HCVtcp with different replicon constructs. (A) Schematic representation of plasmids used for production of HCVtcp. Deduced length of transcribed RNA from each construct is shown on the right. HCV polyproteins from JFH-1 strain are indicated by open boxes. HCV UTRs are indicated by bold lines. The EMCV IRES is denoted by gray bars. Adaptive mutations are indicated by asterisks. F Luc: firefly luciferase gene; P: RNA polymerase I promoter; T: RNA polymerase I terminator. (B) Detection of NS5B and actin in Huh7.5.1 cells transfected with indicated plasmids at 4 day post-transfection. (C) Infectivity of culture supernatants from cells transfected with indicated replicon plasmids along with pCAGC-NS2/JFH1am at 4 day post-transfection.

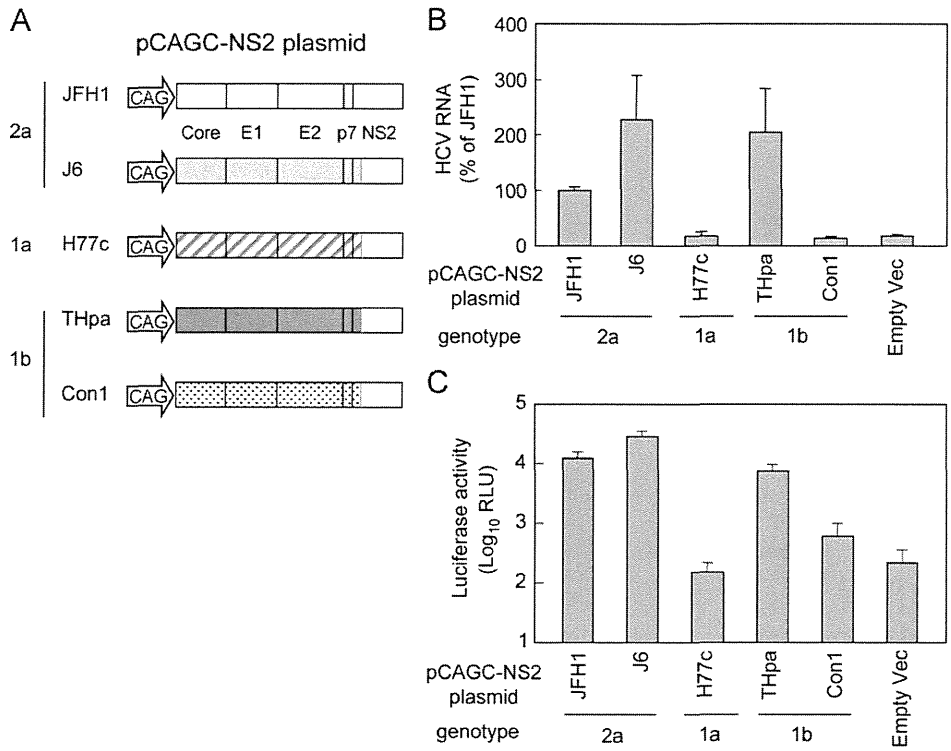

Fig. 3. HCVtcp production with structural proteins from various strains. (A) Schematic representation of plasmids used. HCV polyproteins of JFH-1, J6, H77c, THpa and Con1 strain are shown in the open box, bright gray box, box with diagonal lines, dark gray box and dotted box, respectively. (B) Relative levels of HCV RNA in the supernatant from cells transfected with indicated plasmids along with pHH/SGR-Luc. (C) Luciferase activity in cells inoculated with supernatant from cells transfected with indicated plasmids along with pHH/SGR-Luc at 4 day post-transfection.

pCAGC-NS2/THpa and pCAGC-NS2/JFH1am were used as core-NS2 plasmids for HCVtcp production carrying core-p7 derived from genotypes 1b and 2a (HCVtcp-1b and HCVtcp-2a, respectively). HCVpp derived from JFH-1 and VSVpp were generated and used for comparison. Infection with HCVtcp-1b or HCVtcp-2a was blocked by anti-ApoE antibody in a dose-dependent manner. In contrast, anti-ApoE antibody did not affect infection with HCVpp and VSVpp (Fig. 4A).

The CD81 dependence of infection was also compared between HCVtcp and HCVpp (Fig. 4B). Anti-CD81 antibody inhibited the entry of HCVtcp-1b, HCVtcp-2a, and HCVpp in a dose-dependent manner. The antibody had no effect on VSVpp infection. HCVtcp infection appears to be more sensitive to anti-CD81 antibody when compared with HCVpp infection; more than 60% inhibition was observed at 0.08 μg/mL anti-CD81 antibody for HCVtcp-1b and HCVtcp-2a, whereas approximately 50% inhibition was observed for HCVpp at 2 μg/mL antibody. Neutralization of HCVcc by anti-ApoE and anti-CD81 antibodies was also determined. Antibodies blocked HCVcc infection (Fig. 4C and D), as observed with HCVtcp. These results suggest that ApoE, as well as CD81, play an important role in HCVtcp infection. Thus, HCVtcp may be more useful for evaluating the HCV entry process than HCVpp.

Identification of novel culture-adaptive mutation in NS3 by serial passage of HCVtcp in packaging cells

The HCVtcp system was further applied to analyses of genetic changes during serial passages in target cells. As an initial attempt, supernatants of cells co-transfected with pCAGC-NS2/JFH1am and pHH/SGR were inoculated into Huh7.5.1 cells transiently transfected with pCAGC-NS2/JFH1am. However, infectious titer was lost after repeated inoculation, likely due to low HCVtcp titers and low efficiency of plasmid transduction (data not shown). To overcome this, we utilized recombinant adenovirus vectors (rAdVs) to provide core-NS2. As we were not able to obtain rAdV directly expressing core-NS2, conditional transgene expression based on a Cre-loxP strategy was employed (Kanegae et al., 1995). We constructed an rAdV containing core-NS2 gene downstream of a stuffer DNA flanked by a pair of loxP sites (AxCALNLH-CNS2). When cells were doubly infected with AxCALNLH-CNS2 and the Cre-expressing rAdV, AxCANCre (Kanegae et al., 1995), the Cre-mediated excisional deletion removed the stuffer DNA, resulting in core-NS2 expression under control of the CAG promoter (Fig. 5A). As expected, tightly regulated production of HCVtcp was observed. The cells infected with AxCANCre and AxCALNLH-CNS2 along with transduction of pHH/SGR-Luc produced HCVtcp at high levels. Production of HCVtcp was undetectable when either AxCANCre or AxCALNLH-CNS2 was not infected (Fig. 5B). The Cre-mediated rAdV expression system appears to have yielded considerably higher production of HCVtcp when compared with the settings for plasmid co-transfection.

Supernatants from cells in which core-NS2 was expressed using rAdVs and the subgenomic RNA derived from pHH/SGR replicated were inoculated into cells infected with AxCALNLH-CNS2 and AxCANCre (Fig. 6A). Blind passage was performed by sequentially transferring culture supernatants to cells infected with the above rAdVs. The two independent 10 blind passages (p10) showed virus titers of $>1\times10^6$ IU/mL, which were markedly higher than those of the passage 0 (p0) stock cultures (4×10^4 IU/mL). Side-by-side infection analysis revealed that the HCVtcp p10 #1 achieved a virus titer approximately 36 times higher than that of HCVtcp p0 on the packaging cells at 6 day post-infection (Fig. 6B). Sequencing of the entire replicon in the supernatants at p10 in two independent experiments revealed

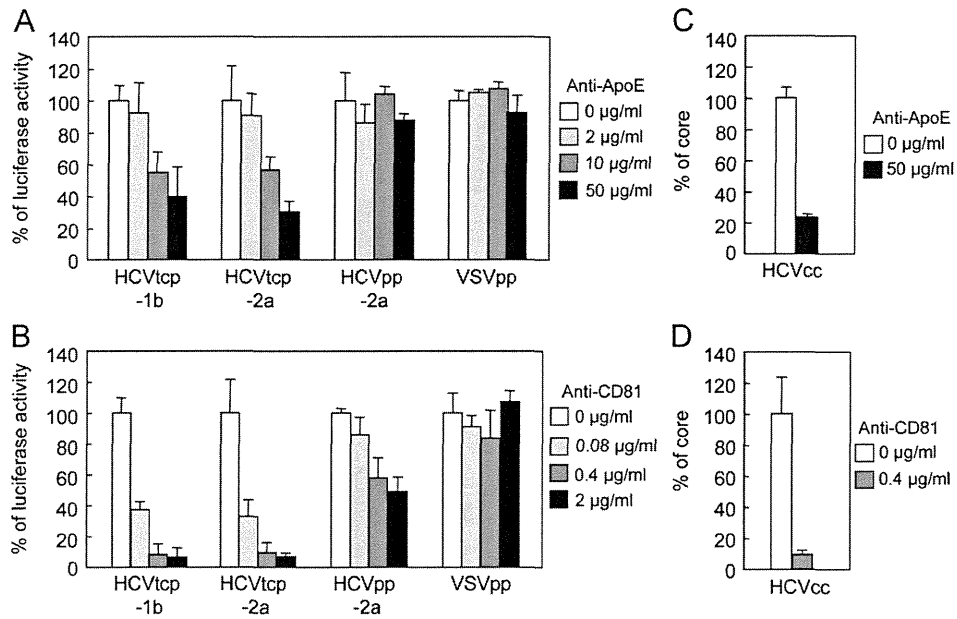

Fig. 4. Effects of anti-ApoE and anti-CD81 antibodies on HCV entry. (A) Aliquots of virus sample were incubated with increasing concentrations of anti-ApoE antibodies for 1 h and were then added to Huh7.5.1 cells. Luciferase activity was determined at 72 h post-infection and is expressed relative to activity without antibodies (white bar). (B) Huh7.5.1 cells were preincubated for 1 h with increasing concentrations of anti-CD81 antibodies, followed by inoculating virus samples. Luciferase activity was determined and expressed as shown in (A). (C) Aliquots of HCVcc were incubated with anti-ApoE antibodies for 1 h and were then added to Huh7.5.1 cells at an MOI of 0.05. Intracellular core levels were quantitated at 24 h post-infection and are expressed relative to levels without antibodies (white bar). (D) Huh7.5.1 cells were preincubated for 1 h with anti-CD81 antibodies. HCVcc infection and measurement of core proteins were performed as indicated in (C).

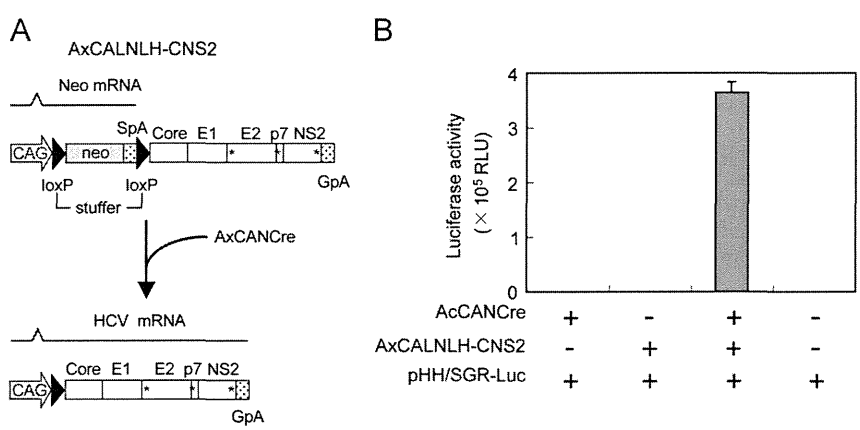

Fig. 5. Transgene activation mediated by rAdVs expressing Cre recombinase under control of CAG promoter. (A) Cre recobminase expressed by AxCANCre recognizes a pair of its target sequences loxP in AxCALNLH-CNS2, and removes the stuffer region resulting in expression of HCV core-NS2 polyprotein by CAG promoter. CAG: CAG promoter; SpA: SV40 early polyA signal; GpA: rabbit b-globin poly(A) signal. (B) Luciferase activity in Huh7.5.1 cells inoculated with 4-day post-transfection culture supernatant from cells transfected with pHH/SGR-Luc, and then infected with indicated rAdVs.

that both passaged HCVtcp had an identical nonsynonymous mutation in the NS3 region (N1586D) (Fig. 6C).

In order to examine the role of NS3 mutation identified on HCV RNA replication and on HCVtcp production, the N1586D mutation was introduced into pHH/SGR-Luc. Luciferase activities of the N1586D-mutated replicon were apparently lower than those of the WT-replicon, thus suggesting that the NS3 mutation reduced viral RNA replication (Fig. 7A). HCV RNA levels in the supernatants of cells transfected with WT- or mutant replicon plasmid along with pCAGC-NS2/JFH1am and luciferase activity in cells inoculated with supernatants from the transfected cells were then determined (Fig. 7B). The viral RNA level secreted from cells replicating the N1586D-mutated replicon was lower than that from cells replicating WT replicon (Fig. 7B, left). By contrast, a significantly higher infectivity of HCVtcp produced from the mutant replicon-cells was observed, as compared to WT replicon-cells (Fig. 7B, right), suggesting that the adaptive mutation increased the specific infectivity (almost 9-fold) of the virus particles. To further determine whether the N1586D mutation affects infectious viral assembly and/or virus release, we used the CD81-negative Huh-7 subclone, Huh7-25 (Akazawa et al., 2007), which may produce infectious particles, but is not susceptible to HCV entry due to a lack of CD81 expression, therefore allowing us to examine viral assembly and release without the influence of reinfection by produced HCVtcp. Measurement of intracellular and extracellular HCVtcp indicated that Huh7-25 cells replicating the N1586D-mutated replicon produced more infectious virus than WT in both supernatants and cell lysates (Fig. 7C). Thus, it can be concluded that the N1586D mutation contributes to enhanced infectious viral assembly, not RNA replication. We could not exclude the possibility that N1586D mutation affects virus release, since the mutation enhanced extracellular virus titers more than did the intracellular titer.